ResearchGate

See discussions, stats, and author profiles for this publication at: https://www.researchgate.net/publication/259846632

ChemInform Abstract: Recent Advances in Small Organic Molecules as DNA Intercalating Agents: Synthesis, Activity, and Modeling

ARTICLE *in* EUROPEAN JOURNAL OF MEDICINAL CHEMISTRY · JANUARY 2014

Impact Factor: 3.45 · DOI: 10.1016/j.ejmech.2013.11.029 · Source: PubMed

CITATIONS
27

READS
351

5 AUTHORS, INCLUDING:

Antonio Rescifina
University of Catania
106 PUBLICATIONS **1,586** CITATIONS

SEE PROFILE

Chiara Zagni
University of Catania
9 PUBLICATIONS **87** CITATIONS

SEE PROFILE

Antonino Corsaro
University of Catania
144 PUBLICATIONS **1,432** CITATIONS

SEE PROFILE

All in-text references underlined in blue are linked to publications on ResearchGate, letting you access and read them immediately.

Available from: Chiara Zagni
Retrieved on: 13 January 2016

European Journal of Medicinal Chemistry 74 (2014) 95–115

Contents lists available at ScienceDirect

European Journal of Medicinal Chemistry

journal homepage: http://www.elsevier.com/locate/ejmech

Invited review

Recent advances in small organic molecules as DNA intercalating agents: Synthesis, activity, and modeling

Antonio Rescifina*, Chiara Zagni*, Maria Giulia Varrica, Venerando Pistarà, Antonino Corsaro

Dipartimento di Scienze del Farmaco, Università di Catania, Viale Andrea Doria 6, 95125 Catania, Italy

ARTICLE INFO

Article history:
Received 26 September 2013
Received in revised form
26 November 2013
Accepted 28 November 2013
Available online 3 January 2014

Keywords:
DNA intercalators
Drug discovery
Docking
Molecular modeling
Anticancer agents
Cancer chemotherapy

ABSTRACT

The interaction of small molecules with DNA plays an essential role in many biological processes. As DNA is often the target for majority of anticancer and antibiotic drugs, study about the interaction of drug and DNA has a key role in pharmacology. Moreover, understanding the interactions of small molecules with DNA is of prime significance in the rational design of more powerful and selective anticancer agents. Two of the most important and promising targets in cancer chemotherapy include DNA alkylating agents and DNA intercalators. For these last the DNA recognition is a critical step in their anti-tumor action and the intercalation is not only one kind of the interactions in DNA recognition but also a pivotal step of several clinically used anti-tumor drugs such as anthracyclines, acridines and anthraquinones. To push clinical cancer therapy, the discovery of new DNA intercalators has been considered a practical approach and a number of intercalators have been recently reported. The intercalative binding properties of such molecules can also be harnessed as diagnostic probes for DNA structure in addition to DNA-directed therapeutics.

Moreover, the problem of intercalation site formation in the undistorted B-DNA of different length and sequence is matter of tremendous importance in molecular modeling studies and, nowadays, three models of DNA intercalation targets have been proposed that account for the binding features of intercalators. Finally, despite DNA being an important target for several drugs, most of the docking programs are validated only for proteins and their ligands. Therefore, a default protocol to identify DNA binding modes which uses a modified canonical DNA as receptor is needed.

© 2014 Elsevier Masson SAS. All rights reserved.

1. Introduction

DNA structure was unknown until 1953 when Watson and Crick determined it through X-ray crystallography obtained by Rosalind Franklin [1]. They described the DNA as a double helix that adopts different three-dimensional conformations although the most common form of the double stranded DNA is the “B” form, characterized by a “right-handed” helix. The backbone of the DNA strand is composed of alternating sugar and phosphate groups with the base linked to each sugar as side chain pair, held by hydrogen bonds between specific pairs of bases. The precise base pairing in their DNA helix model suggested an obvious copying mechanism for genetic material [2]. This discovery opened the door to the belief that DNA was capable of enough structural variety to serve as the molecule of heredity [3]. Therefore, DNA has been identified as a primary target for anticancer drugs, which can change DNA conformation and inhibit duplication or transcription, and is considered one of the most promising biological receptors for the development of chemotherapeutic agents [4]. Two broad classes of noncovalent DNA-binding agents have been identified, the intercalators and the groove binders. Intercalators bind by inserting a planar aromatic chromophore between adjacent DNA base pairs, whereas groove binders fit into the DNA minor groove causing little perturbation of the DNA structure [5,6].

Evidence that there may be important features of DNA structure was reported in 1961 by Lerman who demonstrated that acridine dyes could intercalate between two base pairs of the DNA double helix through non-covalent interactions (hydrophobic, ionic, hydrogen bonding, and van der Waals) [7]. In general, interaction of flat polycyclic aromatic ring molecules with DNA occurs between the π-electron systems of the dye molecule and the heterocyclic rings of the base pairs, and is reinforced by ionic interactions between the positively charged nitrogen atom of an acridine ring and the oxygen atom of the phosphodiester group of DNA [8]. The

* Corresponding authors. Tel.: +39 095 738 5017; fax: +39 06 233 208 980.
E-mail address: arescifina@unict.it (A. Rescifina).

0223-5234/$ – see front matter © 2014 Elsevier Masson SAS. All rights reserved.
http://dx.doi.org/10.1016/j.ejmech.2013.11.029

insertion of an intercalator between adjacent base pairs results in a substantial change in DNA structure, causing lengthening, stiffening and unwinding of the DNA helix. Intercalation requires changes in the sugar-phosphate torsional angles in order to accommodate the aromatic compound, causing separation of the base pairs with a lengthening of the double helix by approximately 3.4 Å and a decrease of the helical twist, unwinding the DNA in the vicinity of the binding site to less than 36° base pair [9]. The presence of an intercalator between two base pairs excludes the access of another intercalator to the binding site next to the neighboring intercalation pocket. Thus, every second (next-neighbor) intercalation site along the length of the DNA double helix remains unoccupied. This phenomena is commonly referred to as the "neighbor exclusion principle" [10,11] and could be explained considering that intercalation results in significant local DNA structural changes with deep alterations in the nucleotide secondary structure [12].

Over the past 45 years, Lerman's observation has spawned a vast literature on intercalators, which have a variety of molecular thicknesses including certain highly potent and effective drugs as well as certain carcinogenic compounds [13]. All of them have chemical structures based on different intercalator frameworks: anthracenes, acridines, anthraquinones, phenazines, quinolones, phenanthridines, phenantrolines, pyrene derivatives, etc.

Molecules that bind to DNA have unique binding site preferences; for example some drugs prefer to intercalate between a 5′-purine–pyrimidine-3′ base step rather than a 5′-pyrimidine–purine-3′ base step (or vice versa) [8]. Slight differences in binding mechanisms determine the sequence preference of the drug, and usually result in variances cytotoxic and pharmacological activity. Although it is well-established that DNA binding is not sufficient to confer cytotoxic activities, interaction with DNA is often considered a necessary criterion for maintaining a cytotoxic effect [14]. However, further studies on some potent DNA intercalators, such as daunomycin Fig. 1 that did not cause inhibition of RNA synthesis, gave rise the doubt that the drug cytotoxicity is not due to what Lerman and other proposed but rather to the interaction with other proteins, found in the 1970's, involved in the control of the shape of DNA. This group of enzymes is called topoisomerases (Topos) [15]. Topoisomerases remove negative and positive superhelical twists from DNA [15] and function by generating transient breaks in the DNA backbone. They can be distinguished in two classes based on the number of strands that they cut [16]. They facilitate the relaxation of supercoiled DNA through a mechanism involving the breakage of a phosphodiester bond of either one strand (Topo I) or both strands (Topo II) of the duplex DNA [17].

In recent years, much attention has been paid to design and synthesize new and efficient DNA-targeted antitumor agents. The goal of this review is to explore the new intercalator drugs synthesized and biologically evaluated in the last few years.

2. Small organic intercalators

Organic intercalators are a class of polyaromatic compounds that can insert or intercalate between two adjacent base pairs of duplex DNA and inhibit nucleic acid synthesis *in vivo* [18]. They are common anticancer drugs in clinical therapy. There are few major modes for reversible binding of molecules with double-helical DNA: (i) electrostatic attractions with the anionic sugar-phosphate backbone of DNA, (ii) interactions with the DNA major groove, (iii) interactions with the DNA minor groove, (iv) intercalation between base pairs *via* the DNA major groove, (v) intercalation between base pairs *via* the DNA minor groove, and (vi) threading intercalation mode Fig. 2 [19].

Intercalating molecules without bulky substituents, such as proflavin, can presumably intercalate without having any significant part of the bound molecule in either the major or minor groove [20]. They are called classical intercalators that bind to DNA duplexes with essentially all of their aromatic system inserted between GpG base pairs from the top and bottom of the intercalation site [21]. Some intercalators carry bulky substituents next to the intercalating moiety, and the substituents are placed in the major and minor grooves when intercalated in duplex DNA. These types of intercalators are called threading intercalators Fig. 2. A threading

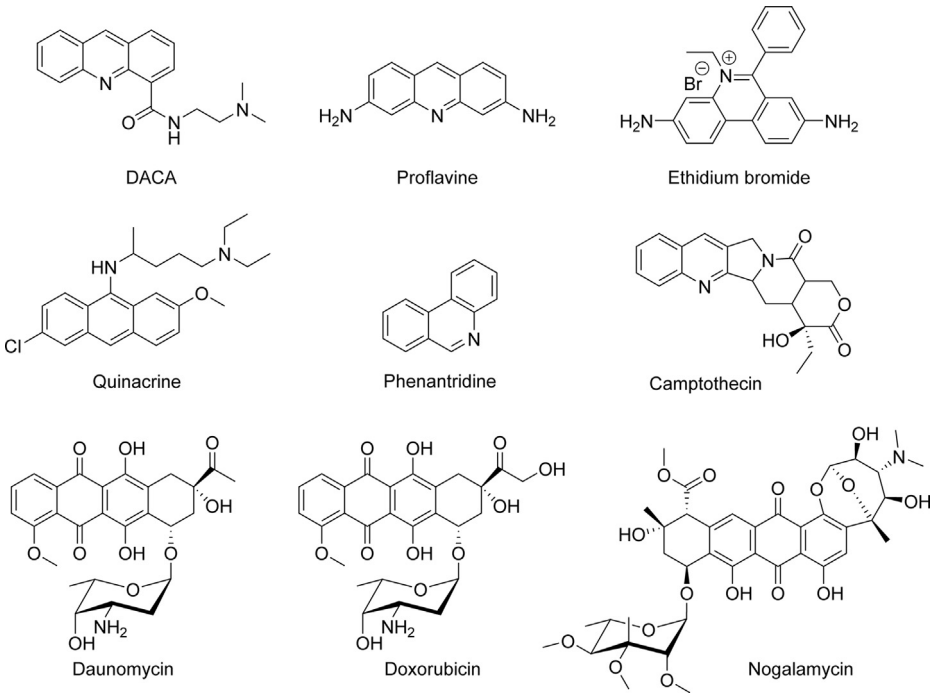

Fig. 1. Selected DNA intercalating agents.

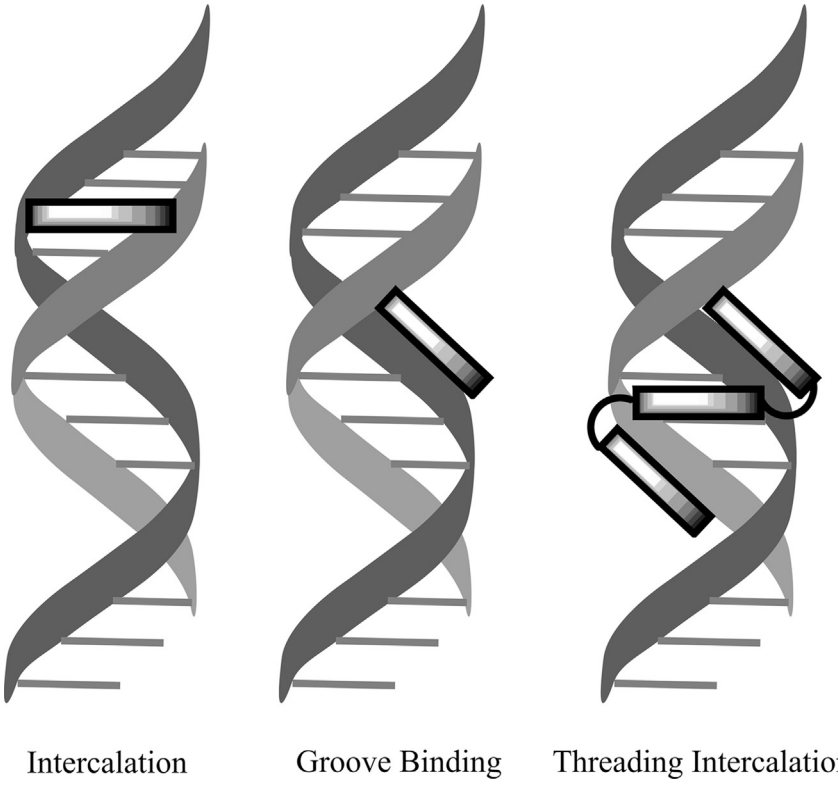

Fig. 2. Schematic representation of classical intercalation, groove binding and threading intercalation mode of DNA.

intercalator occupies and interacts strongly with both the minor and major grooves of DNA simultaneously [22]. The mode, strength and kinetics of binding, meant as the average residence time of the drug at a particular DNA site, are three relevant parameters for the biological activity of DNA intercalators [23].

Other important intercalating drugs such as the anthracyclines, daunorubicin and adriamycin [24–26], phenanthridine derivatives related to ethidium bromide [27], quinacrine [28], and actinomycin [29] have bulky substituents that must be in one groove or the other after the planar aromatic ring of the drugs is bound by intercalation Fig. 1. To date, most evidence supports the location of the bulky groups in the minor groove [30].

2.1. Quinoline and quinoxaline framework derivatives

Quinoline ring system is an important structural unit widely existing in alkaloids, therapeutics and synthetic analogues with interesting biological activities such as antimalarial, anti-inflammatory, antiasthmatic, antibacterial, antitumoral, antihypertensive and platelet derived growth factor receptor tyrosine kinase (PDGF-RTK) inhibition [31–33]. The antitumor activity is due to the intercalation of the aromatic heterocyclic ring between the base pair of DNA and interference with normal functioning of the enzyme topoisomerase II, which is involved in the breaking and releasing of DNA strands [34].

Since peptides exhibit good pharmacokinetic and biological properties there is an increasing interest in the synthetic routes of quinoline containing triazole moiety fused to peptide chain. Recently, Aravinda et al. designed and synthesized quinoline peptidomimetics molecules containing amino acid residues linked *via* 1,2,3-triazole moieties [35]. Compound **3** is obtained by Cu(I)-catalyzed, stepwise variant [36] of Huisgen's classic 1,3-dipolar cycloaddition reaction Scheme (1) [37]. DNA binding studies have been performed by using absorption spectra that revealed DNA binding constant of 4.6×10^4 M^{-1} for compound **3**, which is consistent with the intercalation between the DNA base pairs.

However, diazo compounds are unstable and rapidly release N_2. The synthesized triazole **3** possesses the reactive −N═N− group and is thermodynamically potent activating N_2 release and causing the production of radical when photoirradiated. UV-photolysis of H_2 proved the ability of compound **3** to cleave DNA. Usually, the photosensitizers compounds cleave DNA either initiating a single electron transfer from a base to the triplet state of chromophores,

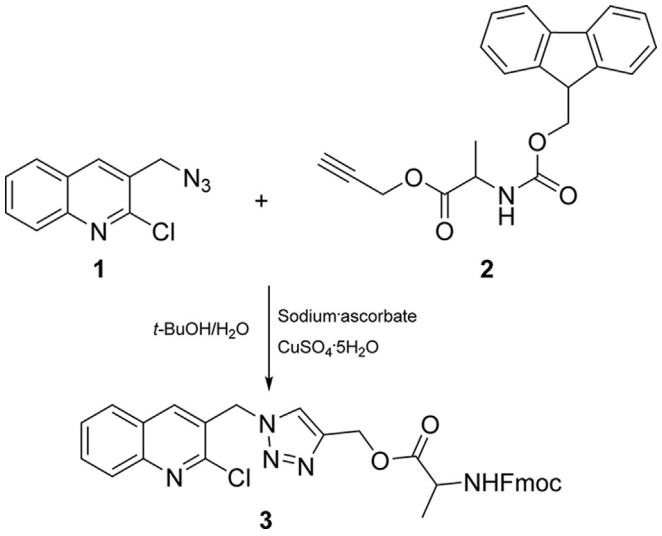

Scheme 1. Synthetic route for the preparation of quinoline linked triazole peptidomimetics.

which often leads to a selective cleavage at the 5′-G of GpG step in duplex DNA, or generating active oxygen species such as •OH radical derived from O_2^- and H_2O_2 [38]. The electrophoretic pattern of DNA treated with compound **3** at different concentration produced DNA strand scission at the same level of H_2O_2 after UV-photolysis. Despite compound **3** has not been tested *in vitro* it can be useful as building block [35].

The *N*-methylated derivative of the anilinoquinazoline skeleton represents a useful chemotype for the development of new DNA-targeted anticancer agent. This class of compounds interacts with double stranded DNA and also present selective recognition of DNA sequences. They can be classified into two major categories, intercalating and minor groove binders [39]. Two different groups of the ether linker at the C-6 and C-7 positions of the quinazoline core, 6,7-dimethoxy- (series A) and 6,7-methylenedioxyquinazoline (series B), have been synthesized and analyzed for DNA binding ability [40]. Binding studies are based on the ability of the drugs to protect calf thymus DNA (ct-DNA) or the synthetic AT polynucleotide [poly-d(AT)$_2$] against thermal denaturation. This technic is used as an indicator of the capacity of the drug to bind DNA and stabilize the DNA double strand [41]. The presence of a methyl group at the anilino nitrogen of quinazoline ring leads to drugs able to stabilize DNA against heat denaturation, while aniline and aryloxy derivatives have a weak DNA affinity as shown by the low ΔT_m values (<5 °C). The 4-anilino-6,7-methylenedioxyquinazoline skeleton is not adapted to stabilize the DNA duplex structure ($\Delta T_m < 5$ °C) unlike the 6,7-dimethoxyquinazoline core (0 °C < ΔT_m < 15 °C) (Table 1).

The halogen (bromine or chlorine) on the aniline ring in *m*-position is more favorable than the *p*-position, whereas the introduction of F, CH_3, or CF_3 apparently reduces the ability to interact with DNA. Introduction of bulky substituents (**12**, **13**) decrease DNA interaction compared to halogen derivatives, while urea group in *m*-position is favorable. The addition of *N*-alkyl substituents (ethyl, propyl, isopropyl) on the anilinoquinazoline nucleus (**16**) did not improve the DNA interaction. However, the introduction of a cationic side chain strongly stabilizes DNA through additional electrostatic interactions with the phosphodiesters groups of DNA. Therefore, the best combination is the bisubstitution by halogens (especially chloride and bromide) and methyl group that reinforce DNA interaction (**17**, **18**). The ability of compound **10** to interact with DNA was further investigated using circular dichroism (CD) and fluorescence measurement showing a binding constant of 3.26×10^4 M^{-1}. The antiproliferative activity of compounds **4**, **5**, **10**, **18** was tested over three cancer cell lines: PC3 (hormono-independent prostate cancer), HT-29 (colon cancer), and MCF-7 (breast cancer). Compound **18**, containing a cationic side chain, emerges as the most cytotoxic agent in this series with IC_{50} (5.6, and 6.8 μM in HT-29 and MCF-7 cell lines, respectively) slightly better than that of compound **10** with a methyl group on the aniline core (6.3 and 9.5 μm on HT-29 and MCF-7 cancers cells, respectively) while the introduction of a cationic side chain tends to favor the antiproliferative activity [40].

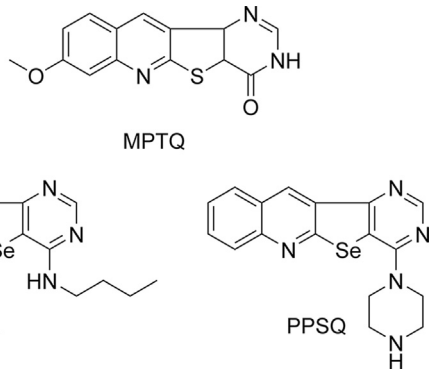

Fig. 3. Structures of MPTQ, BPSQ and PPSQ.

Table 1
Chemical structures, DNA melting temperature measurements and *in vitro* screening results of some *N*-alkyl(anilino)quinazoline derivatives.

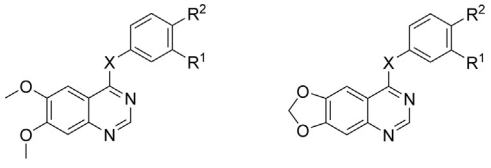

Compd	Series	X	R^1	R^2	ΔT_m (°C) drug/DNA ratio in BPE buffer		Cell lines IC_{50} (μM)		
					ct-DNA	Poly-d(AT)$_2$	PC3	HT-29	MCF-7
4	A	NH	Br	H	0.2	0.4	>10	10.1	4.7
5	A	N–CH_3	Br	H	8.1	12.2	>10	6.1	9.2
6	A	NH	Cl	H	1.8	0.3	–	–	–
7	A	N–CH_3	Cl	H	7.7	12.4	–	–	–
8	A	N–CH_3	H	Br	6.0	10.8	–	–	–
9	A	N–CH_3	F	H	7.3	9.8	–	–	–
10	A	N–CH_3	Br	CH_3	8.4	15	9.5	6.3	9.9
11	A	N–CH_3	Cl	CH_3	8.9	13.7	–	–	–
12	A	N–CH_3	H	NHCONH-(phenyl)	0.4	0.6	–	–	–
13	A	N–CH_3	NHCONH-(phenyl)	H	6.0	9.9	–	–	–
14	B	NH	Br	F	0.3	0.5	–	–	–
15	B	N–CH_3	Br	F	3.6	4.6	–	–	–
16	A	N–CH_2CH_3	Br	CH_3	8.8	13.4	–	–	–
17	A	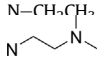	Br	CH_3	9.9	20	–	–	–
18	A	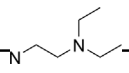	Br	CH_3	14	24.1	>10	5.6	6.8

Structural analogues of ellipticine, pyrimido[4′,5′:4,5]thieno(2,3-b)quinoline-4(3*H*)-one (MPTQ), having a tetracyclic condensed quinolone system, have been synthesized as DNA intercalating Fig. 3 [42]. Biological evaluations revealed that MPTQ is cytotoxic against a wide range of leukemic cell lines such as chronic myelogenous leukemia (K562), T-cell leukemia (CEM) and B-cell leukemic cells (REH and Nalm69) [43]. However the poor solubility and low dissolution rate of the compound in the aqueous gastrointestinal fluids often cause insufficient bioavailability. In order to improve pharmacokinetics of the compound the monohydrochloride of MPTQ (water soluble form) has been synthesized. *In vivo* studies of this compound showed its ability to inhibit tumor progression and improve more than fourfold the lifespan of tumor bearing mice when compared to untreated control animals with tumor. The presence of the small alkyl methoxy group and the substituted oxygen in the aromatic ring of MPTQ may facilitate its entry into the cells and can be responsible for the generation of excessive reactive oxygen free radicals, thereby resulting in cell death. This could explain the dose- and time dependent activation of intrinsic and extrinsic apoptosis pathways induced by MPTQ [42].

Other analogues of ellipticine, pyrimidothieno/selenoloquinolines with a selenium atom in the tetracyclic quinolone system, have been developed as intercalating agents [44]. Is well known that organoselenium compounds such as di, tri, phenyl selenide possess inhibitory effects on different tumors [45]. Two compounds of pyrimidoselenoloquinoline family belonging to two different chemical series have been synthesized and biologically evaluated: butylaminopyrimido[4′,5′:4,5]selenolo(2,3-b)quinoline (BPSQ) and piperazinopyrimido[4′,5′:4,5]selenolo(2,3-b)quinoline (PPSQ) Fig. 3. BPSQ showed significantly higher levels of cytotoxicity in chronic myelogenous leukemia cell line, K562, compared to PPSQ and affects the cell cycle progression by inducing cell cycle arrest at *S* phase and apoptosis. A rational explanation for these significant differences in their biological properties could be the modification in the nature of the side chain. The butylamino substituent of the BPSQ is a hydrophilic alkyl side chain more positively charged in comparison to the piperazino one of PPSQ with a hydrophobic aryl side chain. This may facilitate the efficiency of BPSQ interaction with DNA and probably inhibit replication [44].

A number of 6-aryl-11-iminoindeno[1,2-*c*]quinoline derivatives were designed, synthesized and evaluated for their antiproliferative activity [46]. SAR studies have been conducted for C-2 unsubstituted 6-aryl-11-iminoindeno[1,2-*c*]quinoline derivatives. Substitution of fluorine or methoxy group with an acyclic dimethylaminopropyl group or a pyrrolidin-1-yl ethyl side chain at the C-11 oxime moiety enhanced antiproliferative activity, while the introduction of piperidin-1-yl ethyl on the same position is unfavorable Fig. 4.

Compound **19** exhibited GI_{50} (where GI_{50} is the concentration that cause 50% of cell growth inhibition) values of 0.66, 0.91, 0.61, and 0.70 μm against Hep 3B (hepatocellular carcinoma), A549 (adenocarcinomic human alveolar basal epithelial cells), H1299 (lung carcinoma), and MDA-MB-231 (breast cancer cells), respectively, and was more active than Irinotecan, used as positive control [46]. H-bond donating OH group was more favorable than H-bond accepting OMe group at both C-6 aryl and C-9 positions in which compound **21** and **23** were more active than **20** and **22**, respectively. For the dialkylated 6-aryl-11-iminoindeno[1,2-*c*]quinoline derivatives, aminoalkyl side chain substituted at both C-6 aryl and C-11 positions is more favorable than that of substitution at both C-9 and C-11 positions in which compound **25** was more active than **24**. These 6-aryl-11-iminoindeno[1,2-*c*]quinoline derivatives demonstrated selectivity on subtype of cancer cells. Among six cancer cells tested, MDA-MB-231 and Hep 3B were two of the most sensitive while MCF-7 was the most resistant. Among these 6-aryl-11-iminoindeno[1,2-*c*]quinoline derivatives evaluated, compound **26** was the most active, exhibiting GI_{50} values of 0.64, 0.39, 0.55, 0.67, and 0.65 μm against HepG2 (human hepatocellular liver carcinoma cell line), Hep 3B, A549, H1299, and MDA-MB-231, respectively [46], while compound **27** showed the best activity against Hep 3B.

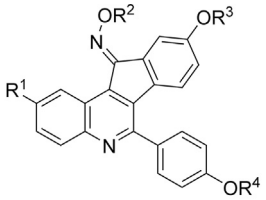

	R^1	R^2	R^3	R^4	Hep 3B IC_{50} (μM)
19	F	$Me_2N(CH_2)_3$-	Me	Me	0.66
20	H	$Me_2N(CH_2)_3$-	Me	Me	3.14
21	MeO	$Me_2N(CH_2)_3$-	H	H	0.67
22	F	N-$(CH_2)_2$-	Me	Me	3.11
23	F	N-$(CH_2)_2$-	H	H	0.64
24	H	$Me_2N(CH_2)_3$-	H	$Me_2N(CH_2)_3$-	5.41
25	H	$Me_2N(CH_2)_3$-	$Me_2N(CH_2)_3$-	H	0.61
26	F	$Me_2N(CH_2)_3$-	$Me_2N(CH_2)_3$-	H	0.39
27	F	N-$(CH_2)_2$-	H	N-$(CH_2)_2$-	0.23

Fig. 4. Chemical structure of some 6-aryl-11-iminoindeno[1,2-*c*]quinoline derivatives.

Similar compounds 6-substituted-9-methoxy-11*H*-indeno[1,2-*c*]quinolin-11-ones have been also synthesized Fig. 5 [47]. SAR studies demonstrated that an alkylamino side chain at C-6 position (**28**) is crucial for cytotoxicity since compounds bearing an aromatic substituent exhibit only marginal antiproliferative activity (**29**). Comparable mean GI_{50} values for **28a** (mean GI_{50} = 3.47 μm) and **28b** (mean GI_{50} = 3.39 μM) over three cancer cell lines, NCI-H460 (Lung), MCF7 (Breast), and SF-268 (CNS), indicate that the cytotoxicity may not be affected by the length of alkyl substituents at C-6 position.

A hydrogen-donating group at C-11 is essential for cytotoxicity since methyl and acetoxy derivatives were inactive. Compound **31a** (with a mean GI_{50} value of 4.17 μm) was more active than **30a** implying that the position of substitution is crucial for cytotoxicity. The most active compound **28b** induces cell cycle arrest at *G2/M* phase *via* cleavage of PARP and activates caspase-3 and caspase-8 activities in a concentration dependent manner. In order to evaluate whether the antiproliferative effect of **28b** was a consequence of DNA intercalation, an *in vitro* DNA unwinding assay was performed. Since compound **28b** enhances the unwinding of negatively supercoiled DNA (form I), as other DNA intercalators, this indicates that it may bind to DNA through intercalation [47].

Bis-intercalator have higher binding capacity and selectivity as well as slower dissociation compared with monointercalator [48]. A new series of potential DNA bisintercalators have been designed by linking the 8-hydroxy-quinoline moiety to the 6-CH_2OH group of

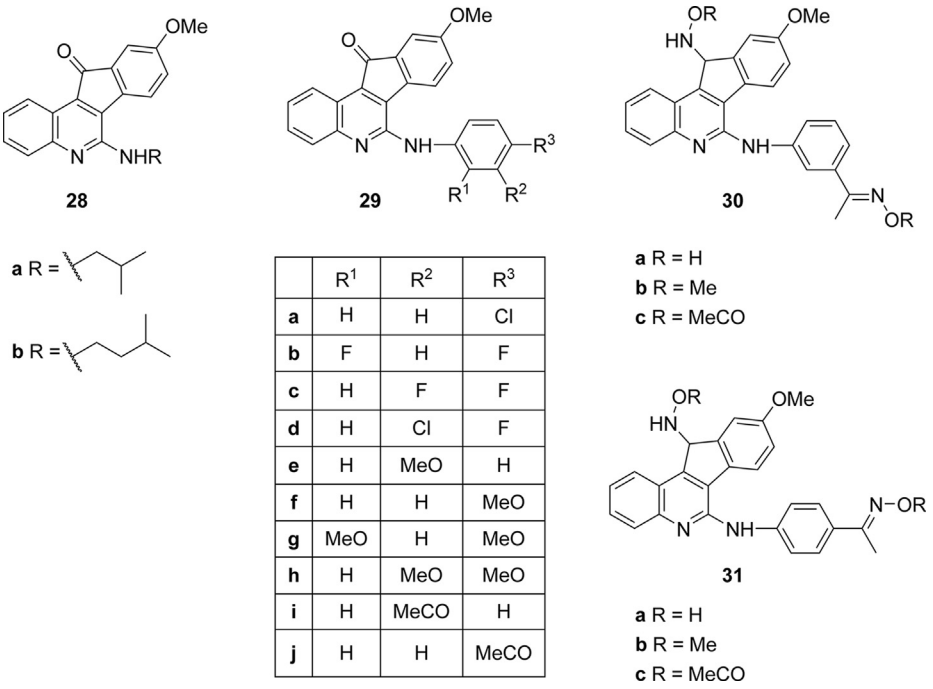

	R^1	R^2	R^3
a	H	H	Cl
b	F	H	F
c	H	F	F
d	H	Cl	F
e	H	MeO	H
f	H	H	MeO
g	MeO	H	MeO
h	H	MeO	MeO
i	H	MeCO	H
j	H	H	MeCO

Fig. 5. Chemical structure of some 6-substituted 9-methoxy-11*H*-indeno[1,2-*c*]quinolin-11-ones derivatives.

glucose and connecting the 1-OH group with various linkers, such as quinol, glycol, and triethylene glycol Fig. 6 [49]. The advantage of using monosaccharides is the high density of the functional groups. Moreover, they are available as single enantiomers and contain multiple sites for attachment of recognition groups [50].

UV absorption and fluorescent emission studies showed the ability of compounds **32** and **33a**–**c** to bind DNA although is not clear the binding mode. To further investigate the interaction between the complexes and ct-DNA a quenching assay based on the displacement of the intercalating drug ethidium bromide (EB) from ct-DNA was assessed. In general, the intensity of EB increases when it intercalates into the base pair of DNA and decreases in the presence of a competitor complex [51,52]. When compounds **32** and **33a**–**c** are added to the solution, the fluorescence intensity of EB bound to DNA at 586 nm showed a remarkable decreasing trend with increased amount of the competitor complex, indicating that some EB molecules were released into the solution after an exchange with the complex, resulting in the fluorescence quenching of EB. The role of glucose group is to enhance the interaction between the compounds and ct-DNA. Of the three target compounds, the 1,4-bis[6-*O*-(8′-quinoline)-*β*-D-glucopyranoside]benzene-1,4-diol (**33a**) seemed to be the most efficient. However, 8′-quinoline-d-glucopyranoside (**32**) exhibited higher affinity with ct-DNA than other bis-intercalators, possibly due to improper linkers or spatial hindrance of the large molecules. The target compounds showed cytotoxic activity against the MDA human breast cancer cell line at concentration of 1 μm [49].

2.2. Phenazine framework derivatives

Several benzo[a]phenazine-5-sulfonic acids have been synthesized as classical DNA intercalators. They present all the necessary characteristic to interact with DNA: a flat aromatic ring capable of insertion in between DNA base pairs and multiple nitrogen atoms important for the degree of planarity to the nucleus and for reducing carcinogenicity and toxicity typical of non-nitrogen polycyclic systems. The compounds synthesized bear structural resemblance of acridine derivatives, known to be strong DNA intercalators [53]. All the compounds have been synthesized by reaction between substituted napthylenedione and *o*-phenylenediamine derivatives in the presence of acid at high temperature. *In silico* studies were carried out in order to predict the pharmacokinetic of the synthesized compounds. The drug likeliness was studied following the Lipinski “Rule of Five” which asserts that all the four parameters values important for a good pharmacokinetic of the compound should assume values multiple of five [54]. According to Lipinski’s rule an orally active drug has no more than one violation of the following criteria:

- its molecular weight is less than 500;
- the compound’s lipophilicity, expressed as log *P* (the logarithm of the partition coefficient between water and 1-octanol) is less than 5;
- the number of hydrogen bond donors (usually the sum of hydroxyl and amine groups in a drug molecule) is less than 5;

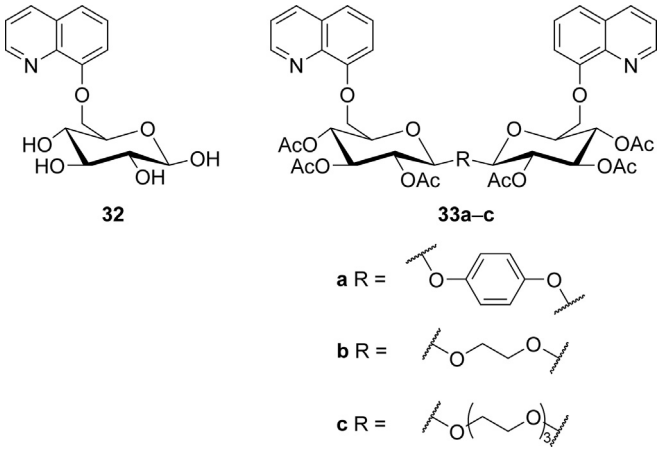

Fig. 6. Chemical structure of 8′-quinoline-D-glucopyranoside and derivatives.

- the number of hydrogen bond acceptors (estimated by the sum of oxygen and nitrogen atoms) is less than 10.

All the synthesized compounds obey the Lipinski rule of 5 regarding molecular weight and number of H-bond donors and acceptor and show log *P* values lower than 3, an optimal balance between good permeability and high solubility.

The presence of different substituents in position 4, 5 and 9 of the benzo[a]phenazine ring influence the pharmacokinetic properties and the *in vivo* activity (Table 2). Compounds **39**–**41**, all bearing a CO group, undergo second phase metabolism and form a conjugated product. The toxicity of these compounds was also predicted using QSAR artificial intelligence techniques indicating that they do not have probability of toxicity except for compound **34**. *In vitro* studies showed that compound **41** is the most active in the series with cytotoxic activity comparable to cisplatinum against HL-60 cell line (human leukemia). The presence of the nitro group in position 4 and 9 decreases the cytotoxic potency (**35** and **36**) whilst reduction of nitro to amino group results in increased cytotoxic activity as well as the introduction of free carboxylic group. Compounds **36** and **41** have been subjected to thermal denaturation studies in order to investigate the interaction with DNA. Both the compounds exhibited DNA binding affinity as showed by large transition in thermal melting points of the DNA [53].

2.3. Indole framework derivatives

Benzo[*c*,*d*]indolone derivatives can easily interact with DNA by hydrogen bond formation between the lactam group of the tricyclic rings and the protein or the backbone of nucleic acid [55]. Moreover, the planarity of the rings system facilitate the embedding of the molecules to DNA base pair. Benzo[*c*,*d*]indol-2(1*H*)-one has three active sites as showed in Table 3. While in the past most energy have been spent in changing sites 1 and 3, Li et al. have focused in the restructuring of site 2 substituting the carbonyl group with a dicyano moiety. This modification allows enlarging the conjugated plane, reducing the electron density and facilitating the binding of the electron-rich DNA. Among the different substituent at the site 1, the amine has been extensively used as an efficient group for the antitumor activity. Nevertheless, the substitution of amino group with electro-deficient chromophore with non-basic side chain (**42**–**48**) did not impact the intercalation and antitumor activity (Table 3). In order to improve the electrostatic interaction with the DNA, unsaturated hydrocarbon **42**–**44** and alkylating groups has been linked to the nitrogen. This modification determined an inhibition of tumor cells growth by cross-linking of basic group. Compound **47**, obtained by substituting the lactam group with an acylamide moiety, has shown the best activity [55].

Table 2
Chemical structures and *in vitro* screening results in HL-60 cell line of some phenazine derivatives.

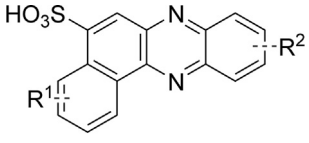

34–41

Compound	R^1	R^2	IC_{50} (μM)
34	H	H	91
35	4-NO_2	H	142
36	H	9-NO_2	124
37	4-NH_2	H	85
38	H	4-NH_2	31
39	H	10-CO_2H	69
40	4-NO_2	10-CO_2H	59
41	H	10-$CON(CH_3)_2$	19

Table 3
Chemical structures of benzo[c,d]indol-2(1*H*)-one derivatives and their antitumor activities against 7721 and MCF-7 cell lines.

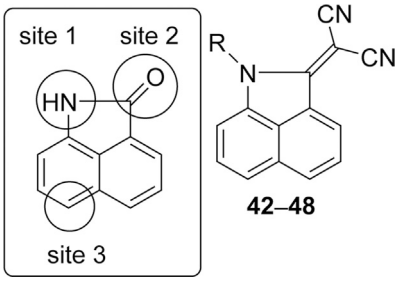

42–48

Compound	R	Cell lines IC_{50} (μM)	
		7721	MCF-7
42	$CH_2C{\equiv}CH$	0.73	12.5
43	CH_2CN	0.26	13.5
44	$CH_2CH{=}CH_2$	0.17	4.73
45	CH_2CH_2Br	0.21	5.38
46	$CH_2CH_2CH_2Cl$	0.35	6.93
47	Ac	0.11	0.003
48	Bz	8.8	15.3

The affinity of the target compounds (**42**–**48**) for ct-DNA was determined by spectroscopic technique and viscosity measurement. The UV–Vis curve of the complex DNA-molecules displayed bathochromic shift and hypochromicity indicating that the compounds are able to intercalate into DNA [56,57]. Binding constant calculated for compound **42** (1.65×10^5 M^{-1}) suggests a good binding ability. Furthermore a quenching assay based on the displacement of the intercalating drug EB from ct-DNA was assessed. When compound **42** was added to the complex of EB and DNA the fluorescence intensity decreased attesting the intercalation of the compound. Compounds **42**–**48** are also able to cleave the close supercoiled DNA into relaxed and open circular form, while compounds **42**–**44** determine a further cleavage into DNA linear form. The hypothesis is that, under photoirradiation, the electron-deficient compounds with the dicyano group would facilitate the electron transferring from DNA to themselves, causing oxidation of DNA, through a charge-transfer mechanism [58].

The *in vitro* cytotoxicity of compounds **42**–**48** was evaluated against MCF-7 cells (human mammary cancer cell) and 7721 cells (human liver cancer cell). Compounds **45** and **46** showed a moderate activity as result of alkylation, and excellent leaving groups (chloride and bromide) are required for cytotoxicity in an alkylation mechanism. Compound **47** exhibited the best activity due to the formation of hydrogen bonds between the acetyl group and DNA bases. The lower activity displayed by compound **48** could be caused by the conjugation of the phenyl with the carbonyl group responsible for the reduction of its competence of forming hydrogen bonds. Despite basic side chains are known to enhance intercalator's antitumor activity, compounds without *N*-dialkyl group basic side chains also exhibited good bioactivity, suggesting that this series of compounds hold different structure–activity relationship (SAR) from traditional DNA intercalators [55].

A molecular docking approach of indole derivatives was conducted by Sechi et al. They synthesized a "two armed" compound, 2,3,6,7-tetrahydro-1*H*-pyrrolo[1,2-*a*]indole-1,8(5*H*)-dione **49**, with

a novel three-ring fused heterocycle functionalized with two chains having a basic terminal group Fig. 7 [59]. The basic chains are able to form cationic head groups, conveniently orientated between the DNA bases (at a distance of 10–12 Å considering the base–base distance, C′–C″, equal to 10.7 Å). The two basic chains bearing a positive charge interact with negatively charged groups (i.e. phosphate groups) through a classic mechanism of intercalation (i.e. between base pairs, from the minor groove) or in the DNA grooves (groove binding). Docking studies have been performed using X-ray crystallography data of the DNA octamer d(GAAGCTTC)$_2$ complexed with N8-actinomycin D (PDB 209D). First the ligand **49**, modeled in the protonate form on both imidazoline rings, was inserted inside (Int) the site, and then was positioned outside (Ext) the intercalating site, in proximity of the base pairs. Thus, an extensive energetic minimization was performed and the values of the calculated free energy of binding, −14.72 (Int) and −13.68 (Ext) kcal/mol, resulted comparable with the ones obtained for the ethidium bromide. Thus, compound **49** resulted a good ligand with a high binding affinity, and can be expected to form a sufficiently stable complex with DNA, probably due to the presence of the protonated amino groups (still protonated in physiological conditions). In order to combine flexibilities of ligand and receptor a new *in silico* approach, called *relaxed complex method* (RCM), was performed [60–62]. First a molecular dynamics (MD) calculation of the DNA octamer, d(GAAGCTTC)$_2$, was conducted. Then the ligand, subjected to docking calculation, was located in the middle 5′-GC-3′ base pair of double stranded DNA by intercalation with the side chains interacting with the phosphate anions. The drug/DNA complex displayed a stable and well-defined configuration during the simulation. Finally, the best complexes found in the docking calculation were improved. Interestingly, although several dynamic conformational changes of the receptor were found, compound **49** remained always docked to the active site. These results confirmed that the tricyclic chromophore is strongly embedded into the DNA helix. Experimental analyses have also confirmed the computational prediction. It is know that, in appropriate condition, the intercalation of small molecules such as ethidium bromide can increase the viscosity of DNA solution [63]. This phenomenon is probably due to the separation of base pairs at the intercalation sites that leads to an elongation of DNA filament. At increasing concentration of compound **49** the relative specific viscosity of DNA solution increases indicating that the compound generate DNA helix extension as a monofunctional intercalator [59].

Further design, synthesis and docking studies have been conducted over indole derivative natural compounds. In particular, in the past years β-carboline-3-carbonylamino acid benzyl ester conjugates have been discovered to be potent anticancer derivatives of natural products with a cytotoxicity dependent on their building blocks including β-carboline-3-carboxylic acid, amino acid and benzyl moieties [64,65]. β-carboline alkaloids such as harmine and its derivatives have been proved to possess highly cytotoxicity against human tumor cell lines by intercalating into the DNA helix and inhibiting DNA topoisomerase I and II. Basing on the concept that many amino acids with functional side chains are capable of making base-specific contacts with more than one type of DNA bases [66], a series of amino acids, containing either nonpolar, acidic, basic, or aromatic sides, differently functionalities with absolute stereochemistry, was introduced into the β-carbolines core [64]. Moreover, amino acid conjugates might target the gastrointestinal transporters involved in the absorption of amino acids and small peptides resulting in improved oral bioavailability [67,68].

Table 4
Docking scores of Trp-Trp-AA-OBz derivatives.

Trp-Trp-AA-OBz	AA	DOCK score	HepG2 (IC_{50} μM)	Trp-Trp-AA-OBz	AA	DOCK score	HepG2 (IC_{50} μM)
50a	Ala	55.6	20.06	**50k**	Met	32.1	52.73
50b	Gly	55.5	17.76	**50l**	Glu	51.2	21.02
50c	Phe	53.0	16.77	**50m**	Asp	37.4	120.78
50d	Leu	30.7	122.83	**50n**	Cys	59.6	11.39
50e	Ile	51.7	22.23	**50o**	Arg	43.0	35.90
50f	Val	61.1	9.49	**50p**	Lys	40.7	30.42
50g	Ser	39.5	46.55	**50q**	Gln	62.1	10.16
50h	Thr	58.6	13.69	**50r**	Asn	49.4	17.95
50i	Tyr	32.1	43.16	**50s**	His	38.4	27.29
50j	Pro	56.5	14.73	**50t**	Trp	41.0	154.03

Finally, it is well documented that Trp-Trp is biologically important either as a dipeptide or as a fragment of some peptides and can be derived by ring-opening of the antitumor active β-carboline-3-carboxyltryptophan benzyl ester suggesting that Trp-Trp-OBz is its pharmacophore. Following this aim, Trp-Trp-OBz was used as a lead, and twenty novel tripeptide benzyl esters, Trp-Trp-AA-OBz, were synthesized as DNA intercalators Fig. 7 [69]. To evaluate the activity of Trp-Trp-AA-OBz **50a**–**t** as DNA intercalators an automated docking toward the cavity of d(CGATCG)$_2$ oligonucleotide (PDB 1D12) was performed [70,71]. The DOCK scores calculated for Trp-Trp-AA-OBz are in the range 31–62, and ten of them fall in the range 51–62, a perfect range considering that the DOCK scores of the intercalators with high *in vivo* anti-tumor activity were from 50 to 60 (Table 4) [65,72].

In vitro anti-proliferation activities of **50a**–**t** were evaluated using carcinoma cell lines. The IC_{50} values, obtained treating HepG2 (human hepatocellular liver carcinoma cell line), S180 (mouse sarcoma cell line), H22 (mouse hepatocellular carcinoma cell line), K562 (human immortalized myelogenous leukemia line) and B16 (mouse melanoma cell line) with compounds **50a**–**t**, are in the range of 8.1–154.0 μm. All the compounds (with the exception of **50d**,**g**,**i**,**k**,**p**,**t**) inhibit the proliferation of carcinoma cells at IC_{50} values lower or equal to that of cytarabine and doxorubicine. This suggests that Trp-Trp-OBz is a good lead and the insertion of amino acid residue into its C-terminus influences the *in vitro* efficacy. In the examination of the intercalation of **50a**–**t** toward DNA, analytical assays were performed using ct-DNA as the model DNA

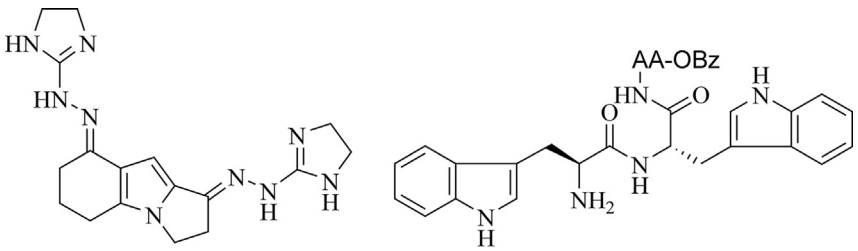

49 **50a–t** Trp-Trp-AA-OBz

Fig. 7. Chemical structure of a two armed derivative of the 2,3,6,7-tetrahydro-1*H*-pyrrolo[1,2-*a*]indole-1,8(5*H*)-dione and the Trp-Trp-AA-OBzl tripeptide template.

and compound **50f** as the model tripeptide. Viscosimetric analysis showed enhanced viscosity of ct-DNA with the increase of the concentration of **50f**. The thermal melting of DNA is widely used to measure the thermostability of the double helix [73], where melting temperature (T_m) is the temperature that induces a 50% increase in the absorbance of DNA solution [74]. Usually, heating DNA at a properly elevated temperature will trigger double strands dissociation with consequent increase of the solution absorbance. The melting curves of ct-DNA alone and ct-DNA plus **50f** showed that the T_m of latter is higher. This indicates that in presence of compound **50f** the double strands of ct-DNA is stabilized. This increased stability of the double helix of ct-DNA can be attributed to the intercalation of **50f**. Further studies, automated docking, UV, CD, and fluorescence, have confirmed that the anti-tumor action of Trp-Trp-AA-OBz occurs by DNA intercalation [69].

2.4. Acridine framework derivatives

Acridine derivatives are one of the oldest and most successful classes of bioactive agents. They are one of the more studied chemotherapeutic compounds, widely used as antimalarial, antiviral, antibacterial, antitumor, antiprotozoal, and antitubercular agents [75–77]. In general, acridines can interact with DNA either *via* intercalation or groove-binding and may block DNA replication, transcription, or DNA repair [78]. Acridine compounds are also able to inhibit topoisomerase I and II enzymes, render a DNA damage, disrupt DNA repair and replication, and induce cell death. Therefore, the planar acridine scaffold is an important pharmacophore and potent fluorescent ligand intercalating between DNA base pairs and is often used in syntheses of antitumor DNA-targeting drugs [79]. The first acridine-based agents, nitracrine [80] and amsacrine, (*m*-AMSA) [81], designed specifically for cancer treatment, were developed in the 1970 Fig. 8 [23]. Amsacrine, introduced into clinical use in 1976 [82], was one of the first drugs recognized to work by forming a ternary complex with DNA and the enzyme topo II, trapping a reaction intermediate termed the "cleavable complex" [83]. Amsacrine has been used over the past three decades to treat patients suffering from acute leukemia and its anti-cancer activity can be attributed to a potent and selective inhibition of topoisomerase II [84].

One of the earliest and most well-known agent possessing a mutagenic effect toward DNA and inhibition of protein synthesis is proflavine [85] Fig. 1. Unfortunately, the use of some acridines has been limited by problems, such as side effects, drug resistance and poor bioavailability. In contrast, thiazolidine compounds have emerged as antineoplastic agents with a broad spectrum of antitumor activity against many human cancer cells [86,87].

Thus, Janovec et al. explored a novel pharmacophore proflavine-dithiazolidinone, linking thiazolidinone skeleton to proflavine structure Fig. 8 [88]. Synthesized compounds **51a**–**e** bear different alkyl substituent in order to investigate whether a proflavine alkyl chain elongation influences the intercalation properties. Analytical studies between ct-DNA and bis-imidazolidines showed binding constants for compounds **51a**–**e** in the range of other intercalator compounds (10^4–10^5 M^{-1}) suggesting that the mechanism of interaction with DNA is little dependent on the length of alkyls, attached to acridine 3,6-positions through the connecting units. The obtained data correspond to the model of acridine skeleton inserted between DNA base pairs while both alkyl chains accommodate themselves in the minor DNA groove and interact with DNA only by weak non-specific interactions. However, the binding constants decreased with a growing bulk of alkyls substituents of both imidazolidinone rings in the order: ethyl > propyl > butyl > pentyl > hexyl.

The synthesized compounds **51a**–**e** have been tested toward L1210 (murine leukemia) and HeLa (human uterus carcinoma) cells lines and compound **51e** was found to be the most active with IC_{50} HL-60 = 2.44 μM (seven-times lower than that of model amsacrine with IC_{50} = 0.34 μm) and IC_{50} L1210 = 4.31 μM (higher than 9-aminoacridine with IC_{50} = 45.0 μM) but lower than that of amsacrine (IC_{50} = 0.05 μM) [88].

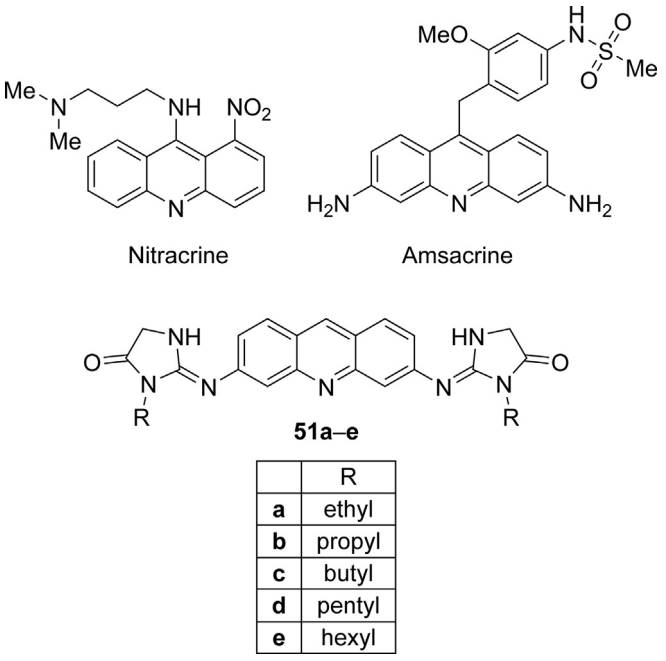

	R
a	ethyl
b	propyl
c	butyl
d	pentyl
e	hexyl

Fig. 8. Chemical structure of some acridine derivatives.

New acridine-thiazolidines derivatives have been synthesized by Barros et al. by coupling acridine and thiazolidine nucleus (**52a**–**d**) [89]. DNA interaction assay results obtained from the dsDNA biosensor clearly demonstrate that compounds **52a**–**d** caused a distortion of the double helix and exposure of the bases to oxidation Fig. 9. A decrease of the oxidation waves of the nucleobases, guanosine and adenosine (using ssDNA) confirmed the interaction of **52a**–**d** with DNA.

The cytotoxicity of the acridine-thiazolidine derivatives was evaluated against several tumor cell lines and amsacrine was used as a positive control. The thiazacridines exhibited relatively high cytotoxicity against colon carcinoma and glioblastoma tumour cell

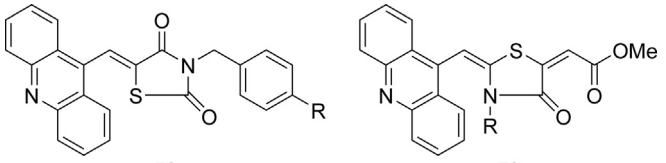

	R
a	Me
b	Br
c	Cl
d	F

	R
a	*s*-butyl
b	*t*-butyl
c	*p*-BrPh

Fig. 9. Chemical structures of acridin-benzylthiazolidione derivatives.

lines, possessing IC_{50} values in the range of 7.4–46.4, 7.2–35.5, 5.8–29.0, and 5.6–58.0 μm for **52a**–**d** respectively, with lower activity compared with amsacrine (IC_{50} values ranging from 0.08 to 3.3 μm). These derivatives possess certain selectivity to glioblastoma while they do not have activity against leukemia, breast carcinoma or normal lymphoblast cells. Although the thiazacridines were shown to be less active and less selective than amsacrine, the selectivity for solid tumor cell lines is interesting [89].

Although anticancer activity of acridines is mainly related to their capacity to bind to DNA, their cytotoxicity may be enhanced by increasing electrophilicity to facilitate the reaction with essential SH groups present in living organisms, especially a main low-molecular thiol, glutathione. Reactivity of acridines with sulfhydryl groups could modify SH-proteins and alter intracellular glutathione redox status, which modulates a lot of cellular events, for example, selective gene expression, DNA synthesis, or regulation of the cell cycle [90,91]. Recently Paulikova et al. synthesized new acridine-thiazolidinone agents that displayed strong cytotoxic activity *in vitro* Fig. 9 [92]. Compounds **53a**–**c** inhibited the growth of cancer cells and induced cellular death of leukemia cell lines, H-60, L1210, A2780, at micromolar concentrations. In particular compound **53c** exhibited the best activity attesting that the *p*-bromophenyl as ring substituent group is favorite compared with *sec*- or *tert*-butyl groups. Moreover, these compounds show high affinity to calf thymus DNA with the binding constants in the range of $1.37–5.89 \times 10^6\ M^{-1}$, one order of magnitude greater than that of daunomycin [92].

2.5. Isoxazolidinyl-PAHs derivatives

Recently, our research group has synthesized isoxazolidinyl-PAHs, a new series of potential, nonionic, DNA intercalators incorporating an isoxazolidine ring in the aromatic planar system of anthracene, phenanthrene, and pyrene nucleus since is known that fused polyaromatic systems of 3–5 rings are desirable to achieve effective intercalation.

The first set of isoxazolidinyl-PAHs (**55**, **56a**–**f**) has anthracene, phenanthrene, and pyrene as polycyclic aromatic system and an isoxazolidine ring that could promote a certain degree of base selectivity assuring a desirable regioselective functionalization of the polycyclic core [93]. The presence of the hydroxyl group at C5 of the isoxazolidine ring plays an important role in the DNA-recognizing region and its ability to form intermolecular hydrogen bonds with the DNA backbone contributes to the formation of a stable complexes [94–96].

Compounds **55** and **56** have been synthesized employing the 1,3-dipolar cycloaddition reaction between nitrones and allyl alcohol by standard procedures [97] and by microwave irradiation (Scheme 2). The reaction was found to be regiospecific, affording 5-substituted isoxazolidines. The low level of *cis*/*trans* stereoselectivity with the *cis* isomer **55** as the major products could be explained by considering that nitrones **54e**,**f** exist exclusively as *Z* isomers, while nitrones **54c**,**d** exist as a mixture of *Z*/*E* isomers.

In order to investigate the ability of these compounds to bind to DNA, UV spectral analysis of a mixture of **55c** and ct-DNA was performed. The red shift of 13 nm for DNA [98] and the binding constant for **55c** with ct-DNA ($6 \times 10^3\ M^{-1}$) were consistent with intercalation. Furthermore, electrophoretic examination of a mixture of **55c** with ΦX174 RF I DNA showed characteristic streaking of the supercoiled species, indicative of intercalation. Additionally, preliminary docking studies of compound **55c** to the B-DNA fragment $d(CGCAATTGCG)_2$ showed that it preferentially intercalates into the DNA AT region where resulting complex seems to be further stabilized by formation of hydrogen bond between the hydroxyl group of the methanol moiety and an oxygen of the phosphate group. The cytotoxicity of all the compounds was assessed *in vitro* against a panel of leukemia (MOLT-3, THP-1) or lymphoma (U-937) as well as against a cell line from normal African green monkey kidney (Vero). The results showed that compound **55e** is the most active toward MOLT-3 leukemia cells and exerts a remarkable enhancing activity on apoptosis caused by anti-fas antibody addition. Furthermore, compounds **55b** and **56b** exhibit specific antiviral effects against the Punta Toro virus [99].

Among the investigated compounds [(3*RS*,5*SR*)-2-methyl-3-pyren-1-ylisoxazolidin-5-yl]methanol (**55c**), a non-ionic pyrene derivative, exhibited promising cytotoxic and apoptotic properties. The binding of **55c** to DNA has been widely investigated using different techniques. UV–Vis experiments showed hypochromic effects accompanied by the formation of tight isosbestic points upon binding of **55c** to polynucleotides poly-$d(AT)_2$ and poly-$d(GC)_2$. The related binding constants correspond to $6.8 \times 10^3\ M^{-1}$, $6.0 \times 10^3\ M^{-1}$ and $1.5 \times 10^3\ M^{-1}$ for ct-DNA, poly-$d(AT)_2$ and poly-$d(GC)_2$, respectively. The fluorescence emission intensity of **55c** was slightly quenched by ct-DNA, essentially unaffected by poly-$d(AT)_2$

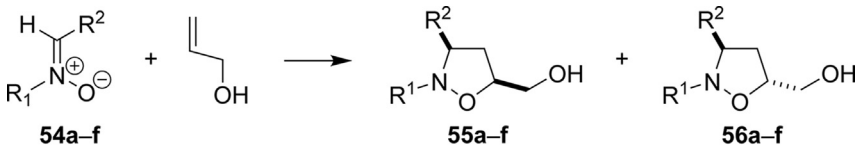

	R^1	R^2		R^1	R^2
a	Me	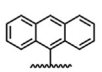	**d**	Bn	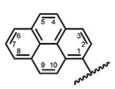
b	Me		**e**	Bn	
c	Me	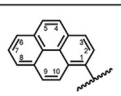	**f**	Bn	

Scheme 2. Synthesis of some isoxazolidine-PAHs.

and efficiently suppressed by poly-d(GC)$_2$. All the data suggest an intercalative binding mode of compounds **55c** with ct-DNA and poly-d(AT)$_2$ and only a slight intercalation with poly-d(GC)$_2$. Docking studies revealed a common binding with the chromophore that intercalates between the staked base pairs and the isoxazolidine ring lying along the major groove. As seen for other similar compounds, hydrogen bond is formed between the hydroxyl group of the **55c** methanol moiety and the oxygen of the phosphate group. The preferential binding selectivity of **55c** for intercalation in AT-rich regions is probably attributable to steric hindrance between the *N*-methyl group of **55c** and the 4-amino group of the cytosine in the GC sites [100].

The second generation and an isosteric series of pyrenyl- and phenanthryl-isoxazolidine (**60**–**63**) have been synthesized using the 1,3-dipolar cycloaddition methodology (Scheme 3). This series of compounds has shown a better role in the DNA recognizing region because of the ability to form favorable intermolecular hydrogen bonds with the DNA backbone.

The cytotoxicity of compounds **58**–**63** was evaluated *in vitro* against human cervical carcinoma (HeLa), human lung cancer (A-549), a panel of leukemia (Molt-3, THP-1) and lymphoma (U-937), as well as against normal African green monkey kidney (Vero) cell lines. Compounds **61b** ($IC_{50} = 11$ μM) and **62b** ($IC_{50} = 9$ μM) showed high level of cytotoxicity against A-549 cells, but lower than actinomycin D, a well-known intercalating agents. Whereas for compounds **61** and **62** the *cis*/*trans* configuration has a weak influence on the cytotoxicity, with the *cis* isomer that is more active than the *trans* one, in the case of the succinimidic derivatives **60** and **63** the *trans* isomer exhibited greater activity.

Compound **62b** was used as model to investigate the DNA intercalation. Electrophoretic examination of compound **62b** with ΦFX174 RF I DNA, UV spectral analysis and titration experiment indicates that the examined compound intercalates into ct-DNA with a binding constant of 9.6×10^4 M^{-1}, 14-fold greater than that with compound **55c** ($K_B = 6.8 \times 10^3$ M^{-1}). To further investigate the intercalation mode, the supramolecular complexes of compound **8b** with DNA have been studied by molecular modeling methodology. The binding energies, calculated by docking study, suggested that compound (3*R*,5*S*)-**62b** is the most affine displaying a preference for intercalation into the poly-d(AT)$_2$ fragment from the minor groove while compounds **60** and **63** showed a marked preference for the GC nucleobases with an insertion from the minor groove. Moreover, the affinity for AT nucleobases is 18-fold greater than that of its precursor (3*R*,5*S*)-**55c** ($\Delta\Delta G_{Bind} = 1.57$ kcal/mol) [101].

A third generation of isoxazole-, isoxazolinyl-, and isoxazolidinyl-PAHs, as DNA-intercalator, has been also synthesized using the procedure previously described (Scheme 4) [99,101].

The cytotoxicity of compounds **65**–**68**, **71** and **72** was assessed *in vitro* against carcinoma cell lines (HeLa, A-549, Molt-3, THP-1, U-937) as well as normal African green monkey kidney (Vero) cell lines. Compounds **65b** and **65d** showed good cytotoxicity against A-549 cells with IC_{50} of 7 and 4 μm, respectively. In particular, the new derivative **65d** showed an improved cytotoxic activity over the previously reported compounds and lower toxicity compared to actinomycin D with IC_{50} for Vero cells of 42 and 11 μm, respectively, slightly more higher than the first and second series of isoxazolidinyl-PAHs **55c**, **60b**, **61b**, **63b** [99,101]. Analogously to the first and second isoxazolidine series the *cis*/*trans* configuration has a weak influence on the cytotoxicity, with the *trans* isomer more active than the *cis*. The binding constant of compound **65d** with ct-DNA is 1.7×10^5 M^{-1}, 25-fold greater than that obtained for compound **55c** ($K_B = 6.8 \times 10^3$ M^{-1}). The titration of compound **65d** with polynucleotides poly-d(AT)$_2$ and poly-d(GC)$_2$ gave a K_B of 1.6×10^5 M^{-1} and 0.3×10^5 M^{-1}, respectively. All the new compounds, with the exception of **66c** and **68d**, that equally intercalate with AT and GC nucleobases from minor groove, show a clear preference for the poly-AT fragment intercalating from the minor groove as observed by investigation of supramolecular complexes. The

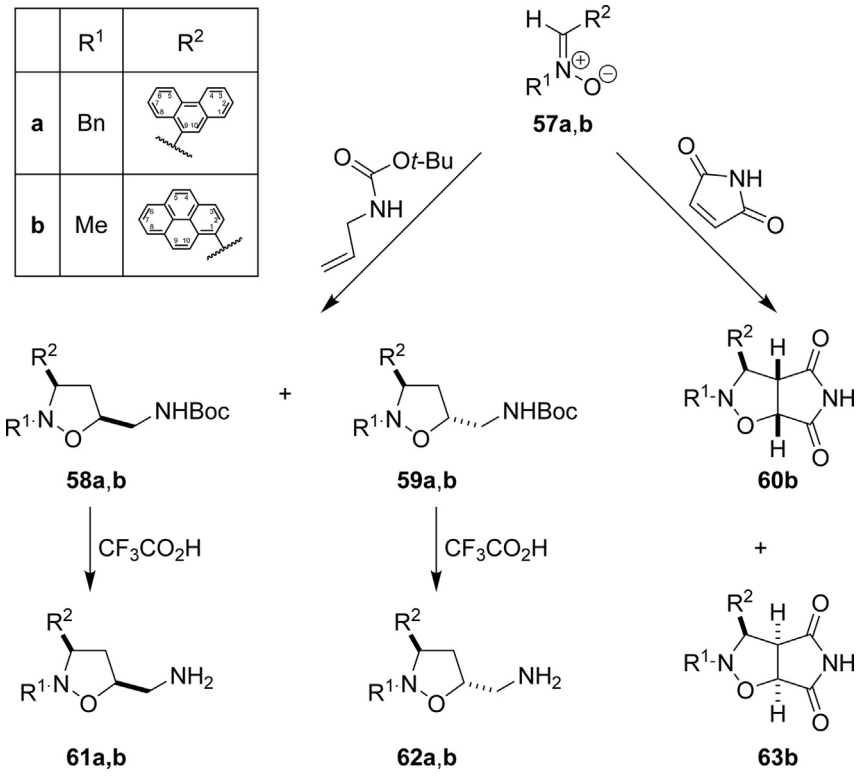

Scheme 3. Synthesis of isoxazolidine-PAHs **58**–**63**.

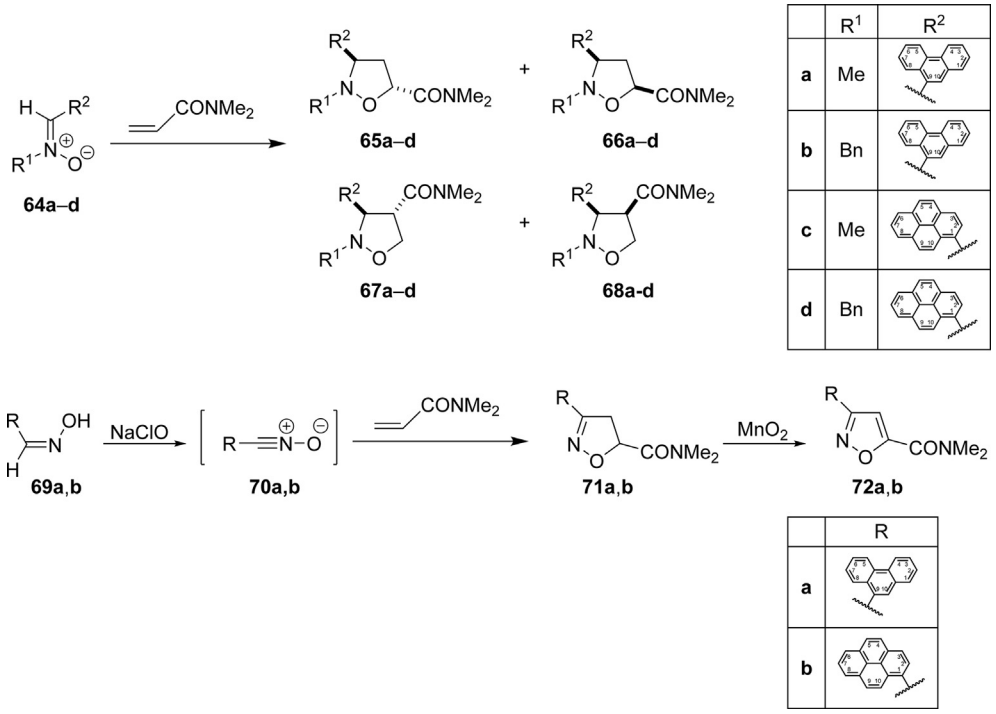

Scheme 4. Synthesis of some isoxazole-, isoxazolinyl-, and isoxazolidinyl-PAHs.

affinity of compound **65d** for AT nucleobases is 46.9- and 3.3-fold greater than that of its precursors (3R,5S)-**55c** (ΔG_{Bind} = 2.28 kcal/mol) and (3*R*,5*S*)-**61b** (ΔG_{Bind} = 0.71 kcal/mol), respectively. Δ^2-isoxazolinyl **71a** and the isoxazole **72a**, bearing the 9-phenanthryl moiety, exhibited a good IC_{50} activity (greater than **55c**) [102].

Recently, it has been reported that silver complexes act as antimicrobial agents, interacting with DNA, and that Ag^+ is able to form a metal-mediated base pair complex with the cytosine–cytosine mismatches (C–Ag^+–C) that stabilizes DNA duplex [103]. The double function (DNA intercalator and Ag^+ biosensor) can be performed by integrating appropriate functional groups within the same molecular structure. Therefore compound **55c** has been modified by substituting the methyl group linked to the nitrogen of the isoxazolidine with a hydroxybenzyl group Fig. 10. Compounds **73a**,**b** have been tested *in vitro* against a panel of tumor cells (A-549, Hela, Molt-3, THP-1, U-937) and showed a good activity while Vero cells were more resistant. In particular the *cis* isomer **73a** resulted more active (IC_{50} = 2 μM toward A-549) of the *trans* **73b**.

Incubation of **73a** with ΦFX174 RF I followed by electrophoretic examination, showed characteristic streaking of the supercoiled species, indicative of intercalation. Supramolecular complexes of synthesized compounds with DNA have been investigated by molecular modeling methodology. The results of docking calculations showed compound (3*R*,5*S*)-**73a** intercalates into poly-d$(GC)_2$ from minor groove engaging three hydrogen bonds, one between the hydroxymethyl oxygen atom and the aminic hydrogen of G8 nucleobase and the others two between the phenolic and hydroxymethylic hydrogens with the backbone rybosyl oxygens of G8 and C9 nucleobases, respectively. The insertion of 2-hydroxybenzyl functionality on the isoxazolidine nitrogen atom leads to a better interaction with the base pairs with respect to the intercalation observed with the protonated aminomethyl derivative. Compound **73a** showed also a relevant selectivity towards Ag^+ cation. Noteworthy, as Ag^+ belongs to transition-metal ions, which usually quench fluorescence emission, this result appears interesting because only few fluorescent sensors for detecting silver ion have been reported to date [104].

2.6. Threading intercalators

The first molecule known as threading intercalation was Nogalamycin Fig. 1, an anthracycline antibiotic that threads between the phosphodiester backbones and interacts with both strands in the minor and major grooves of the DNA [105]. Nogalamycin is a dumbbell-shaped molecule constituted of a planar aglycone with bulky substituents on the opposite sides of the chromophore. Nogalamycin acts threading through the duplex. The aglycone moiety is intercalated between the base pairs, the nogalose is positionated in the minor groove, and the fused bicyclo amino sugar in the major groove [106].

Recently, Howell et al. synthesized 9-(6-aminohexyl)aminoacridine carboxamides as new threading intercalators based upon the well-studied acridine-3- or 4-carboxamides structure [107]. These molecule are composed by an acridine skeleton, responsible for the binding to the DNA duplex, a linker whose length is important to correctly locates the attached groups in the vicinity of DNA, and an aliphatic/aromatic systems or short peptide that are able to interact with DNA. Different assays have been performed in order to study the ability of compounds **74a**–**b** to intercalate into DNA. The binding assay revealed that compounds **74a**–**b** bind to DNA with a binding constant of $3.10 \times 10^7\ M^{-1}$ and $9.83 \times 10^6\ M^{-1}$, respectively, 17-fold

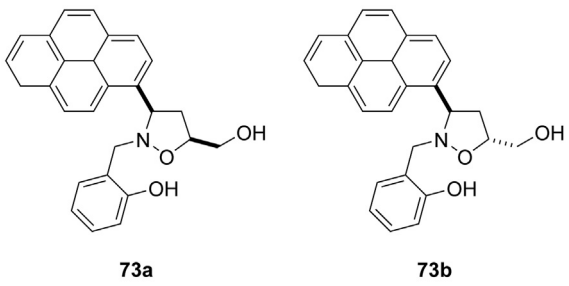

73a 73b

Fig. 10. *N*-Hydroxybenzyl-isoxazolidinyl-PAHs **73a**,**b**.

higher that of 9-aminoacridine (1.81×10^7 M^{-1}). The greater activity of compound **74a** compared to **74b** is probably due to the better steric fit of **74a** within the major groove. The cytotoxicity was assesses against the human leukemia cell line HL60 (Table 5). Also in this case the regioisomer with the carboxamide group in position 4 has better activity than the substituted one in position 3, exhibiting an IC_{50} of 0.45 and 38.3 μM, for compound **74a** and **74b** respectively.

The higher activity of compounds with aliphatic chain rather than aromatic substituents probably comes in part from the electrostatic interaction possible with the protonated primary amine. In fact, electrostatic interactions play a role in binding as the dansyl group (**76a** and **76b**) maintains the binding affinity of compound **74a**–**b**. Whit the introduction of a small peptide (**79**) to the **74a** structure a decrease of less than 10-fold in binding affinity ($K_B = 3.68 \times 10^6$ M^{-1}) is detected. This decrease could arise from the presence of the C-terminal glutamic acid, which is likely to be deprotonated at pH 7.0, although the binding would be enhanced by the protonated histidine [107].

2.7. Miscellaneous framework intercalators

Recently, barberine (**80**), an isoquinoline alkaloid, has been characterized to possess antineoplastic effect due to its ability to intercalate into DNA, bind to the minor groove and inhibit the topoisomerase II enzyme [108,109]. Many derivatives of barberine (**80**) have been synthesized by introducing different substituents in the ring. In particular, 9-substituted compounds showed an improvement in the Topo II interaction where 12-bromo analogues were weaker enzyme poison but stronger DNA binding agents [110]. The binding affinity of barberine (**80**) with CT DNA (3.64×10^6 M^{-1}) is improved in 9-*O*-substituted berberine series. The presence of *N*-aryl/aryl–alkyl amino carbonyl methyl substituent at the 9-position enhances DNA-binding probably through hydrogen bonding and electrostatic interaction with DNA. The binding affinity of the analogs was dependent on the length of the side chain (as shown in Table 6) while further chain elongation gradually reduces the binding affinity. The highest binding affinity was detected for compound **81** which is three times more active than barberine (**80**) [111].

Psoralen, belonging the family of furocoumarin, forms covalent bonds with the double-stranded DNA according to these two processes: intercalation into DNA and photochemical reaction with DNA by UV irradiation at 365 nm [112]. Recently, psoralen has been immobilized with β-cyclodextrin (PβCD) with various methylene linkers by Yamada et al. Fig. 11 [113]. The synthesized PβCD is able to intercalate into the double-stranded DNA and form DNA–PβCD conjugated material with covalent bonding by UV irradiation at 365 nm.

The DNA–PβCD conjugated material has both the functions of intercalation and encapsulation into the intramolecular cavity. The encapsulation property has also the potential for use the DNA–PβCD conjugated as accumulation of harmful compounds that increases with the length of the linker between psoralen and cyclodextrin.

DNA cleavage agents have a potential application as anticancer drugs [114,115]. Usually they are metal transition complexes but recently new metal-free DNA cleaving reagents have been developed [116–118]. In particular, bis-tacnorthoamide derivatives with one or two tacnorthoamide (tacnoa) units linked by a spacer containing anthraquinone (**85**–**86**) or with two tacnorthoamide units linked by an alkyl (1,6-hexamethylene) spacer without anthraquinone have been synthesized from triazatricyclo-[5.2.1.04,10]decane (**87**) Fig. 12 [119].

Fluorescence and CD spectroscopy assays, using ct-DNA, suggested that compounds **85**–**87** have strong DNA binding affinity, with binding constants of 1.3×10^7 M^{-1}, 0.8×10^7 M^{-1} and 8.0×10^5 M^{-1}, respectively. The DNA cleavage promoted by **85**–**87** and parent tacnoa under physiological conditions was studied by agarose gel electrophoresis, which demonstrates that the introduction of anthraquinone in compound **85** results in a large enhancement of DNA cleavage activity. The higher DNA cleavage activity exhibited by compound **85**, compared with **86**, is probably due to the cooperative catalysis of the two positively charged tacnoa units. Further studies suggested that the cleavage mechanism of compound **85** would be *via* a hydrolytic pathway by cleaving phosphodiester bond of DNA.

The bacterial metabolites chartreusin and elsamicin A Fig. 13 are known to bind to DNA, inhibit topoisomerase II and cause apoptosis through various downstream processes [120]. Common to both of these polyketide glycosides is the pentacyclic aglycone chartarin, a

Table 5
Chemical structures and *in vitro* screening results in HL-60 cell line of some threading intercalators.

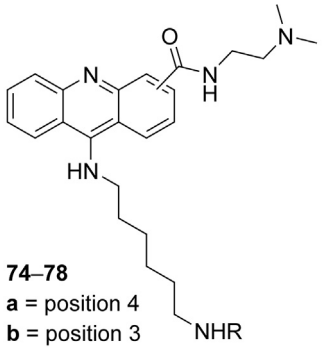

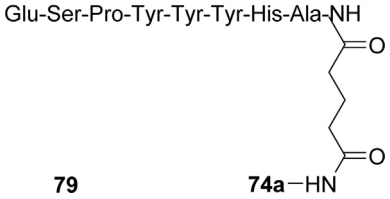

Compound	R	IC_{50} (μM)
74a	H	0.45
75a	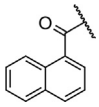	3.5
76a	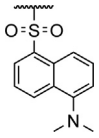	2.1
77a	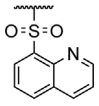	16
78a	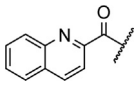	22.6

Table 6
Chemical structures and binding constant values for barberine and its derivatives.

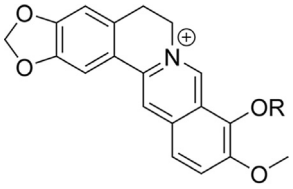

80–83

Compound	R	$K_B \times 10^5$ M^{-1}
80	CH_3	3.64
81	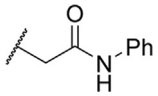	9.14
82	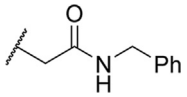	6.72
83	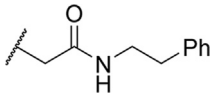	5.98

chromophore capable of intercalating into DNA and causing radical-mediated single-strand scission of DNA [121].

However, the clinical use of these compounds is hampered by severe side effects. In order to overcome these disadvantages, a novel vinyl-substituted chartreusin analogue has been synthesized [122]. Cytotoxic assay against K-562 and HeLa cancer cells resulted in slightly lower activity of compound **88** compared to chartarin. In contrast, the activity of vinylchartreusin (**88**), evaluated under photoinduced condition against colon adenocarcinoma cell line (HT-29), proved to be 12-fold higher (IC_{50} = 0.6 μM) than without light (IC_{50} = 7.1 μM) and signs of apoptosis were observed after irradiation for 2 h, while the activity of native chartreusin was not

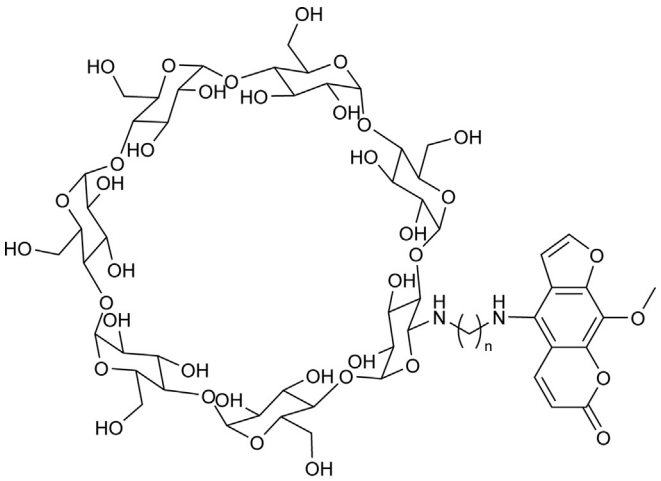

84 n = 2
n = 6
n = 12

Fig. 11. Molecular structure of psolarene-immobilized cyclodextrin with various methylene linkers.

affected by treatment with light. Finally, electrophoretic mobility assay (EMSA) results strongly suggested that compound **88** is able to form A covalent adduct with DNA.

α-(3-Hydroxy-4-methoxyphenyl)-*N*-phenyl-α-amino-phosphonate (HMPAP) Fig. 14, an analogue of α-amino acids well-known as antibacterial, antioxidant and antitumor agent, has been investigated for its ability to bind to DNA [123]. Fluorescence and UV–Vis absorption spectroscopies revealed that HMPAP could bind to ct-DNA with high affinity through intercalation binding.

The fluorescence intensity of HMPAP strongly increased with the addition of ct-DNA probably due to the stacking of the planar aromatic groups between adjacent base pairs of ct-DNA, while wavelength shift was not observed. The competitive binding assay with EB was carried out and showed a decrease in the fluorescent intensity of DNA–EB complex, after the addiction of HMPAP, with a quenching extent of 43.2%, indicating that the compound is able to compete with EB in binding to DNA. UV–Vis absorption spectroscopy studies revealed a decrease in the absorption upon addiction of ct-DNA. The hypochromicity suggests HMPAP may bind to DNA by intercalation mode as result of a strong interaction between the electronic states of the chromophore and those of DNA bases [124]. Isothermal titration calorimetry (ITC) study also confirmed that HMPAP can bind to DNA with a binding constant in the range of 1.01–3.04 × 10^4 M^{-1}. Despite the binding constant being not excellent, these studies can provide important insight into the design of new HMPAP drugs.

A new challenge regarding the application of DNA-targeting drugs is the spatial and temporal control of the drug–DNA interaction, since the regulation of the drug activity will enable a highly selective chemotherapeutic approach. One example of this regulation would be the selectively activation of molecules, with low ability to intercalate into DNA, to compounds able to bind DNA. In the past years photochromic spiropyran [125], dithienylethene [126], azobenzene [127], or chromene derivatives [128], which may be activated in a reversible reaction and photoactive substrates that are transformed irreversibly into DNA-binding ligands upon irradiation [129], have been synthesized with this aim. This process where one component of the photochromic equilibrium represents a DNA-targeting drug formed *in situ* only upon irradiation is of particular interest since allows the photocontrolled dosage of a drug in close vicinity to its target [130].

Recently, Ihmels et al. have developed a similar system that may be used for the *in situ* generation of DNA intercalators [131]. They synthesized a styrylbenzothiazole derivative **89** with low affinity towards DNA that, upon photoinduced electrocyclization and oxidation, is converted into the product **90** exhibiting the two characteristic features of a DNA intercalator: an extended heteroaromatic π system and a permanent positive charge (Scheme 5A). Photometric titration of ct-DNA to compound **89** revealed only a very weak interaction while the quinolinium derivative **90** showed a strong hypochromic effect along with a bathochromic shift of the absorption maximum (Δλ = 14 nm), characteristic of a strong ligand–DNA interaction with a binding constant of 1.7 × 10^5 M^{-1}. In order to explain the mode of binding a viscometric assay has been performed and revealed that compound **90** induces change of viscosity characteristic of DNA intercalators, whereas groove binding ligands do not increase the viscosity of DNA solutions.

Ihmels et al. synthesized a new photochromic systems consisted of a *N*-methylphenanthrolinium-annelated spirooxazine derivative **92** where, upon irradiation at 350 nm, the spirooxazine moiety is transformed into the corresponding photomerocyanine one that allow compound **93** bind to DNA (Scheme 5B) [130]. The association of compounds **92** and **93** with DNA was examined by CD, absorption spectroscopy, fluorescent intercalator displacement and viscometric titration. The photometric titrations indicate more than

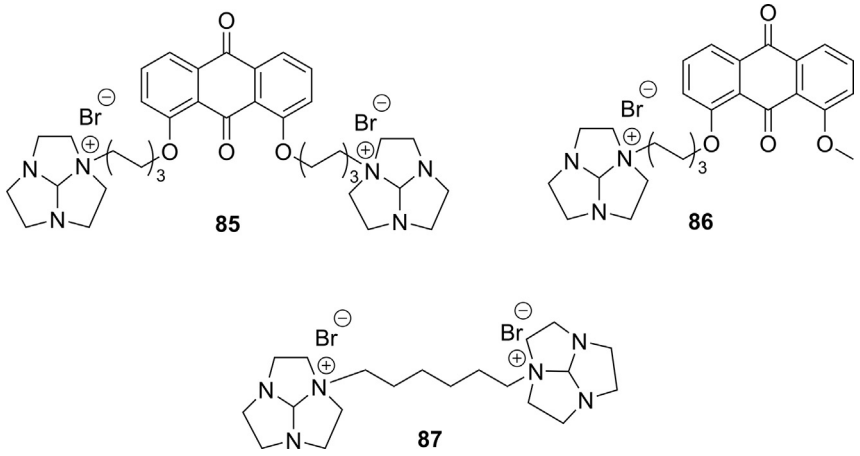

Fig. 12. Chemical structure of tacnorthoamide derivatives.

one binding mode, apparently depending on the ligand–DNA ratio. While the spirooxazine does not exhibit a measurable affinity to DNA, compound **93** exhibits a titration profile characteristic of an intercalative binding mode, in agreement with the viscometric titrations. The experiments with synthetic polynucleotides poly-d(AT)$_2$ and poly-d(GC)$_2$ provide some evidence for a preference of the ligand **93** towards GC-rich DNA sequences. These analyses showed that the binding constant (7.9×10^4 M^{-1} with ct-DNA) of compound **93** is relatively low compared with other established DNA intercalators. This could be explained taking in consideration that has been demonstrated the increase of the cross-sectional thickness of a DNA intercalator reduces its affinity towards the nucleic acid [132]. Since the thickness of the compound **93** is higher than compound **92**, specifically in close proximity to the phenanthrolinium part, this may lead to a significant steric hindrance of the ligand–DNA interaction. Nevertheless, the spirooxazine–photomerocyanine system could be a promising platform to develop effective photoswitchable DNA ligands.

3. Docking and molecular modeling

Nucleic acids can take a wide array of complex shapes as their single, double, triple, and even quadruple nucleotide interactions permit multifaceted conformations to form. From the very beginning of nucleic acid study with the physical models of Watson and Crick, abstraction and modeling have played a significant role in the

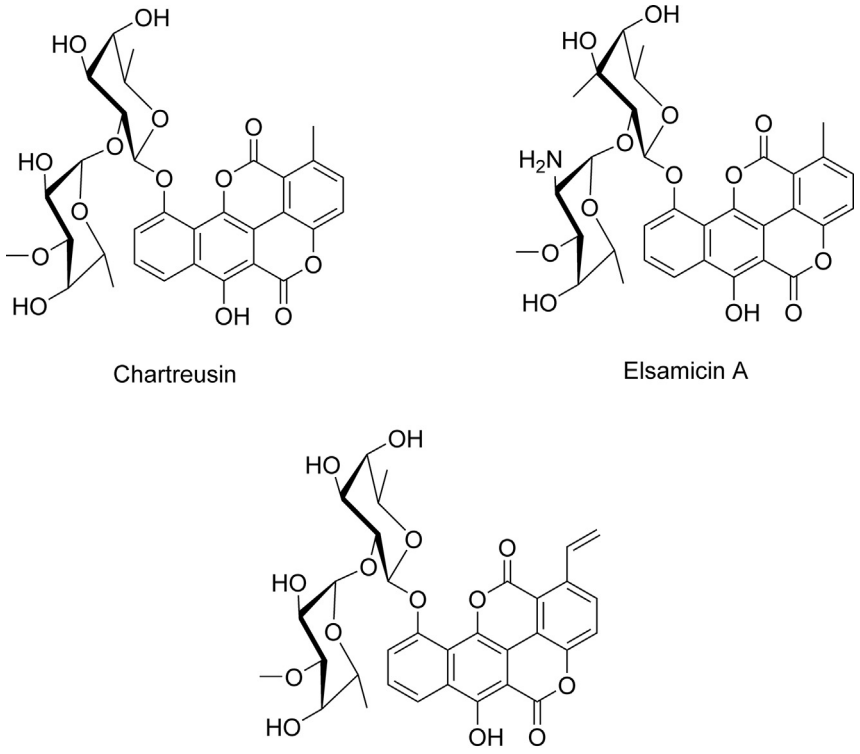

Fig. 13. Chemical structures of chartreusin analogues.

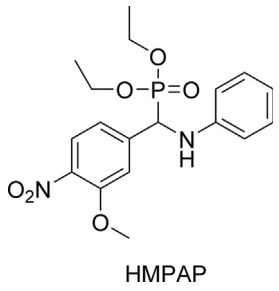

HMPAP

Fig. 14. Chemical structure of HMPAP.

understanding of DNA and DNA–ligand interactions. These physical models gave rise to mathematical concepts and techniques to study complex configurations. Just as these models describe DNA molecules ranging from the micro to the macroscale, the methods used in their simulation are also suited for an array of length and timescales.

As with the sentiment of Box – "Remember that all models are wrong; the practical question is how wrong do they have to be to not be useful" [133] – it must be remembered that nucleic acid models are only approximations; each model therefore, must be evaluated to determine to which biological systems it is best suited before it becomes "not useful" [133]. The simulation of nucleic acids is now a mature field [134] and modeling techniques are powerful tools for the understanding and description of their forms and functions, although careful consideration must be utilized when choosing a nucleic acid model and method. In this paragraph we will succinctly outline the state of art to *in silico* investigate DNA-intercalating ligand interactions, i.e. docking and MD simulations, and the latest findings.

Despite DNA being an important target for several drugs, most of the docking programs are validated only for proteins and their ligands. As well-known, nucleic acids differ from proteins due to unique structural features such as high density charge and helix chiral geometry. Also, nucleic acids do not present a single and well-defined binding site, as occur with most of the proteins, and offer more solvent exposed binding pockets [135]. As a consequence, this leads to the question of whether docking programs validated for proteins can also produce reasonable results in ligand–DNA docking. This issue has been recently approached by Holt et al. [136], who has shown that AutoDock and Surflex can accurately reproduce the crystal structure of several ligands (minor groove binders and intercalators) bound to DNA, within a resolution of approximately 2 Å.

However, although self-dockings (i.e., using the original crystallographic target) are considered useful as a first indication of docking accuracy, they have proved to provide little information about accuracy in real drug discovery [135]. Indeed, the employment of docking techniques to elucidate unknown DNA binding mechanisms, without any conclusive previous experimental data, remains a challenge and the main issue is: when it comes to the docking of ligands whose binding mode to DNA remains unknown, which oligomer conformation should be used as target?

In the tentative to answer to this question Ricci and Netz [137] performed self-dockings (i.e. a docking of cocrystallized ligands to their protein targets) and cross dockings studies, employing AutoDock 4.0 software, between two DNA ligands (netropsin, a minor groove binder and ellipticine, an intercalator) and four distinct receptors: 1) crystallographic DNA without intercalation gap (the dodecamer d(CGCGATATCGCG)$_2$ complexed with netropsin, PDB code 1DNE); 2) crystallographic DNA with intercalation gap (the hexamer d(CGATCG)$_2$ complexed with ellipticine, PDB code 1Z3F; 3) canonical B-DNA; and 4) modified B-DNA with intercalation gap. These studies pointed out that AutoDock 4.0, besides being efficient in self-dockings, it is able to correctly reproduce the binding mode of a ligand docked with canonical DNA (cross docking), provided that the target DNA presents an artificial intercalation gap; this suggests that the AutoDock 4.0 score function is efficient to evaluate ligand–DNA interactions at least in a qualitative way. On these bases a default protocol was suggested to identify DNA binding modes which uses a modified canonical DNA, with gap, as receptor. Precisely, a canonical B-DNA, generated with X3DNA [138], is modified to include an intercalation gap positioning the ligand between two selected base pairs, parallel to the base ring, and minimizing the complex by the steepest descent method, with the GROMOS 53A6 force field. The resulting complex, without the ligand, furnish the modified B-DNA that is used as a "receptor" for docking. The best AutoDock parameters, with respect accuracy/rate of simulation, utilizing the more accredited Lamarckian Genetic Algorithm (LGA), are 25 runs with an initial population of 50 individuals, a maximum number of 5×10^7 energy evaluations, and a maximum number of 27,000 generations. Mutation and crossover rates of the population were set to 0.02 and 0.80, respectively, for the Global Search routine, and with translational, orientational, and torsional step size set to 0.2 Å, 5.0° and 5.0°, respectively, for the Local Search routine that utilizes the pseudo Solis and Wets

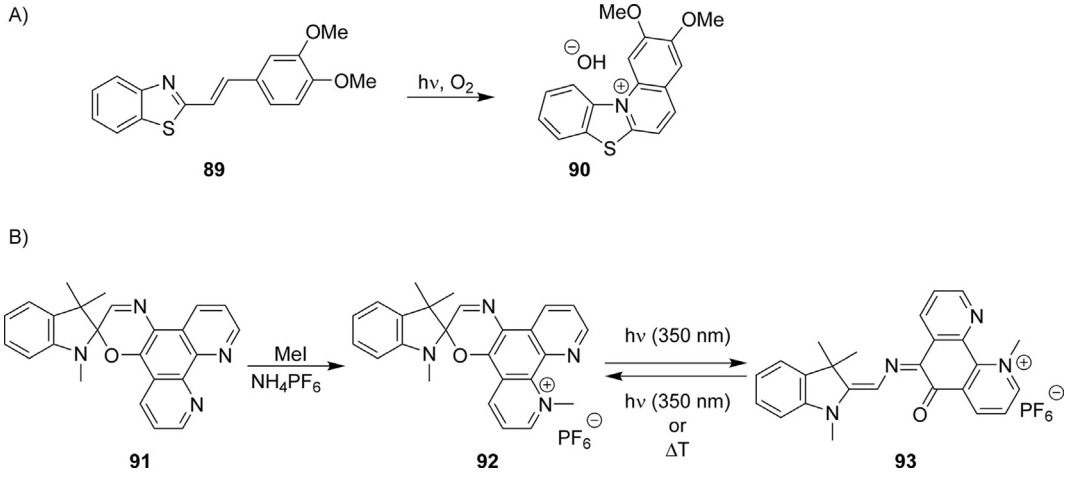

Scheme 5. A) Photoreaction of the styrylbenzothiazole derivative **89**. B) Synthesis of spirooxazine **92** and photochromic equilibrium between **92** and the photomerocyanine **93**.

algorithm. Default values were applied to all other parameters. Finally, this protocol was successfully validated in the prediction of the correct binding modes of both a symmetric and an asymmetric, optically active, Tröger bases.

Enormous progress has been made in terms of the use of MD applied to DNA simulations; the improvements in hardware and software have led to spectacular increases in the length of trajectories that, nowadays, are in the scale of microseconds and go to the milliseconds one thus entering in the biologically relevant timescale. This has resulted in the necessity of a new parameterization of the most renowned AMBER 99 force field to correct the artifactual unfolding of DNA, due to the neglect of long-range effects, and the unbalanced α/γ transitions founded in simulation above 30 ns. The newest AMBER force field, parmbsc0, yields stable trajectories in the multi microsecond scale [139]. At the same time, a valid simulation protocol utilizing water as explicit solvent, potassium as counterion to achieve neutrality, and an additional quantity of KCl to simulate the physiological conditions (0.15 M), within periodic box conditions (PBC), has been developed and optimized [140–143].

These improvements in the use of MD simulations applied to nucleic acids has led to important results in the study of the mechanism of interaction involved in the intercalation of a specific ligand between the DNA base pairs.

This mechanism has been well described in many papers [63,144–151], and four major mechanistic approaches have been proposed, which differ in their kinetic micro-steps. In one of these proposed mechanisms, the two-step one, the intercalator electrostatically binds externally to the DNA in a fast process, followed by a slow insertion step to the intercalation site [145–147] while in the three-step mechanism the intercalated complex forms a secondary intercalated complex, either *via* a geometrical change within the intercalator itself, or by the intercalator moving from intercalation site to another intercalation site without re-entering the solvent [148–150].

Currently, a computational simulation may not be able to run long enough to reach a transition state relative to the intercalation process, but there are some methods by which a system may be driven to a transition state, such as adiabatic melting, cross-correlation analysis [152], replica exchange molecular dynamics (REMD) [153], forced motions along a known trajectory [154], metadynamics [155] and umbrella sampling [156]. Some of these methods require prior knowledge of the mechanism being studied, and although guesses may be made to test hypothetical transitions, the results would then be suggestive but not conclusive.

In 2010, Monaco has succeeded, for the first time, in grabbing, fortuitously, a transition state for the intercalation of ethidium cation to the d(AGGATGCCTG)$_2$ decamer, during a 500 ps MD simulation [157], starting from the unbound state. This simulation seem to shows a two-step mechanism, where the ethidium does not move away from its externally bound position but twists in place and slips into an intercalation site created in response to steric and electrostatic forces resulting from the twisting motion of the charged ethidium. This final intercalation step, then, suggests that the intercalator is involved in creating the intercalation site rather than passively waiting for such a site to occur spontaneously, despite the fact that significant fluctuations in DNA rise are known to occur at room temperature. Therefore, this simulation [158] provides support for the two-step mechanism of ethidium interaction over the three-step one. A more detailed MD study was conducted on the interaction of daunomycin with DNA, starting from the bound state, employing both metadynamics and umbrella sampling strategies [159,160].

The results of these two independent approaches are found to be consistent and reveal a passage from the groove to the intercalation site involving a metastable intermediate and two transition states. In the metastable intermediate state, daunomycin is partially intercalated at a 5′-CpG-3′ step, opening up a wedge angle between the two base pairs on the minor-groove side and bending DNA toward the major groove. In particular, the optimal pathway involves initial binding to the minor groove with minimal DNA deformation (with a binding free energy of roughly −10 kcal/mol using the umbrella-sampling simulations with a physiological salt concentration). An activated process (requiring roughly 6.5 kcal/mol under the same conditions) causes the drug to rotate and to partially insert its planar anthraquinone moiety into a wedge formed between two successive base pairs. This intermediate state lies in a shallow free energy well (with a depth of roughly 1.5–2.0 kcal/mol). Crossing a small free energy barrier is therefore sufficient to achieve full intercalation. From a kinetic point of view this process is partially compatible to the three-state model of Chaires [150].

The existence of an intermediate state, where the drug is partially intercalated and DNA is wedged open on the minor-groove side and bent away from the drug, is of particular interest when are considered other DNA interactions. From a therapeutic point of view, it is interesting to note that when DNA kinking toward the major groove is stabilized, e.g. by cisplatin binding to successive bases in the major groove, this can enhance protein binding in the minor groove, notably by HMGB1, which can then block DNA repair and induce cell apoptosis. This suggests that if it were possible to significantly stabilize the intermediate metastable state by chemically modifying daunomycin, or related drugs, this might provide an interesting new direction for drug development.

Contemporaneously, Wu et al. studied, by MD simulations, the intercalation mode between doxorubicin and two DNA examers, d(CGATCG)$_2$ and d(CGTACG)$_2$, starting from the unbound state [161]. The MD trajectories for the intercalative pathway pointed out an alternative route to the standard assumptive rise-insertion mechanism that well accord to the five-step kinetic model proposed by Rizzo et al. [151].

The intercalation pathway of d(CG**AT**CG)$_2$ was: (a) unbound state → (b) minor groove binding → (c) initial insertion → (d) deep insertion with two bases flipping out → (e) deep insertion with one base flipping out; slightly different, the intercalation pathway of d(CG**TA**CG)$_2$ was: (a) unbound state → (b) breaking base pair C1–G12 upon initial ligand insertion → (c) flipping out of C1 and deep ligand insertion → (d) wrong hydrogen bond paring between C1 and G12 → (e) flipping out of G12 → (f) good paring between C1 and G12.

This putative base-flipping mechanism has the following two advantages: 1) the DNA deformation energy due to the local base-flipping (−20.6 kcal/mol) is less than that of the global stretching (−23.1 kcal/mol); 2) the DNA deformation penalty is overcome by the favorable binding energy during the intercalation process. In other words, the drug induced flipping lowers the drug insertion free energy barrier suggesting that the base pair flipping might be an obligatory step or at least an important alternative pathway leading to the intercalation.

Finally, Mukherjee and Sasikala conduced an in-depth study on the intercalation of proflavine [162,163], one of the simplest intercalators with a planar geometry because of which the static picture obtained from its intercalated crystal structure does not provide any indication about the intercalation and de-intercalation pathway.

Most of the kinetic studies on the intercalation of proflavine propose that the process comprises two steps: a fast bimolecular outside binding, faster than a few tenths of a millisecond, followed by a slow intercalation that arise in the range of a few milliseconds [164], irrespective of the nature of DNA as well as the base sequences [165].

So, utilizing a well-temperated metadynamics method, have been determined the molecular thermodynamics and kinetics

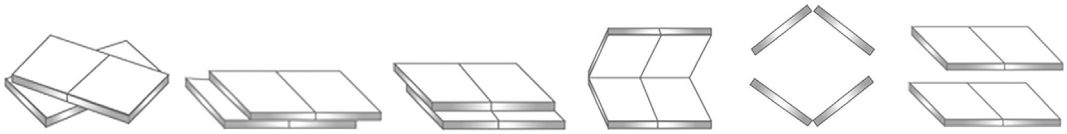

Fig. 15. Movements of base pairs during intercalation; from left to right: twist, slide, shift, roll, negative cup, rise.

involved in the intercalation, de-intercalation and dissociation processes of proflavine through both the major and minor grooves of the DNA. Astonishingly, the results indicate that the intercalation and de-intercalation pathways of proflavine proceed through the major groove side. However, intercalation is mostly dominated by the stable pre-intercalative minor groove-bound state, which builds up in few nanoseconds and slowly leaks to the intercalated state over a timescale of milliseconds through the major groove side. This long timescale is in excellent agreement with experimental kinetic results and the free energetic components for the stable states and barrier heights are also in good agreement with experimental findings.

Moreover, the mechanism along the minimum free energy path reveals that intercalation happens through a minimum base stacking penalty pathway where nonstacking parameters (Twist → Slide/Shift) change first, followed by base staking ones (Buckle/Roll → Rise) Fig. 15. Another time, this mechanism defies the natural fluctuation hypothesis and provides molecular evidence for the drug-induced cavity formation one.

This study predicts, furthermore, that the intercalated structure may not be as static as appears in the crystal structure and proflavine would likely change its orientation frequently even in the intercalated state. Entropy and desolvation energy are shown to play a major role in the kinetic process. Both de-intercalation and dissociation are energy driven processes and groove-bound states are found to be entropically unfavorable. Therefore, the designing of a drug would eventually encounter two seemingly opposite effects: on the one hand, an increased drug–DNA stacking interaction is required to stabilize the intercalated state and, on the other hand, a less stable pre-intercalated state needs to be designed to make the kinetics faster.

4. Conclusions

Over the past many years, the search for new cytotoxic intercalators has mainly followed classical approaches: structural modifications to conventional molecules, new natural products, potential synthetic compounds and chemical conjugates. With the aim of reviewing the most studied and the new classes of DNA intercalators we propose the most significant molecules synthesized in the last years. A particular attention has been paid on chemical-physic studies as well as *in vitro* biological evaluation and docking analysis of the mentioned compounds. In our opinion, must be carried further efforts to develop a method of docking, with relative scoring functions, that is able to predict in a quantitative way the binding constant of the ligand–DNA interaction. For this purpose we have recently undertaken a study, designed to improve the prediction and the correct positioning of the intercalator, that consist to create the site of intercalation using only the planar polycyclic portion of the intercalator, perform a preventive docking to identify the best configuration of the intercalating agent in the formation of the complex, proceed with a 5 ns MD of the complex thus obtained, optimize the last frame and, finally, re-docking. Using this procedure on complexes with known binding constant is possible to build a line/curve $K_{B\text{-exp}}/K_{B\text{-calcd}}$ that allows to extrapolate the correct K_B from the calculated one. At the moment we have investigated 35 complexes getting a straight line with a correlation coefficient of 0.98.

Moreover, MD simulations have definitively ruled out the mechanism of cavity formation based on the natural fluctuation hypothesis and provide molecular evidences for the drug-induced one. As regards, instead, the mechanism of interaction involved in the intercalation of a specific ligand between the DNA base pairs, MD calculations have highlighted the possibility of coexistence of both two- and three-step models, depending on the complexity of the intercalator moieties, and coming to postulate the possibility, in the case of very simple intercalators, that the whole intercalative process can be mostly dominated by a stable and fast-originating pre-intercalative minor groove-bound state which slowly pass to the intercalated one through the major groove side.

These findings could help in the design of new drugs: 1) the existence of an intermediate state with the drug partially intercalated stabilize the kinking of DNA toward the major groove that in turn enhance protein binding in the minor groove blocking DNA repair and inducing cell apoptosis; this suggests that if it were possible to significantly stabilize the metastable intermediate by chemically modifying the intercalator this might provide an interesting new direction for drug development; 2) while an increased drug–DNA stacking interaction is required to stabilize the intercalated state, a less stable pre-intercalated state needs to be designed to make the kinetics faster.

Although in the last two years DNA G-quadruplexes have emerged as new molecular targets for therapeutic intervention with a particular focus on anticancer, the copious literature upon classic DNA intercalators (about 111 papers from January 2009 to May 2013, the time covered by this review) indicate that the interest in this topic is still alive, and further studies may lead to a better understanding of the mechanisms involved in the process of intercalation pointing the way for the design of more selective and potent intercalators.

References

[1] J.D. Watson, F.H. Crick, Molecular structure of nucleic acids: a structure for deoxyribose nucleic acid, J.D. Watson and F.H.C. Crick. Published in Nature, number 4356 April 25, 1953, Nature 248 (1974) 765.
[2] J.D. Watson, F.H. Crick, Genetical implications of the structure of deoxyribonucleic acid, Nature 171 (1953) 964–967.
[3] F. Leone, Genetics: the Mystery & the Promise, TAB Books, Blue Ridge Summit, PA, 1992.
[4] L. Li, W. Cao, W. Zheng, C. Fan, T. Chen, Ruthenium complexes containing 2,6-bis(benzimidazolyl)pyridine derivatives induce cancer cell apoptosis by triggering DNA damage-mediated p53 phosphorylation, Dalton Trans. 41 (2012) 12766–12772.
[5] J.B. Chaires, Drug–DNA interactions, Curr. Opin. Struct. Biol. 8 (1998) 314–320.
[6] H. Ihmels, L. Thomas, Intercalation of organic ligands as a tool to modify the properties of DNA, in: J.-I. Jin, J. Grote (Eds.), Materials Science of DNA, CRC Press, Boca Raton, 2011, pp. 49–76.
[7] L.S. Lerman, Structural considerations in the interaction of DNA and acridines, J. Mol. Biol. 3 (1961) 18–30.
[8] K. Nakamoto, M. Tsuboi, G.D. Strahan, Intercalating Drugs, in: Drug–DNA Interactions, John Wiley & Sons, Inc, 2008, pp. 119–208.
[9] N.J. Wheate, C.R. Brodie, J.G. Collins, S. Kemp, J.R. Aldrich-Wright, DNA intercalators in cancer therapy: organic and inorganic drugs and their spectroscopic tools of analysis, Mini Rev. Med. Chem. 7 (2007) 627–648.

[10] P.J. Bond, R. Langridge, K.W. Jennette, S.J. Lippard, X-ray fiber diffraction evidence for neighbor exclusion binding of a platinum metallointercalation reagent to DNA, Proc. Natl. Acad. Sci. U. S. A. 72 (1975) 4825–4829.
[11] S.N. Rao, P.A. Kollman, Molecular mechanical simulations on double intercalation of 9-amino acridine into d(CGCGCGC) X d(GCGCGCG): analysis of the physical basis for the neighbor-exclusion principle, Proc. Natl. Acad. Sci. USA 84 (1987) 5735–5739.
[12] B.A.D. Neto, A.A.M. Lapis, Recent developments in the chemistry of deoxyribonucleic acid (DNA) intercalators: principles, design, synthesis, applications and trends, Molecules 14 (2009) 1725–1746.
[13] L.B. Hendry, V.B. Mahesh, E.D. Bransome Jr., D.E. Ewing, Small molecule intercalation with double stranded DNA: implications for normal gene regulation and for predicting the biological efficacy and genotoxicity of drugs and other chemicals, Mutat. Res. -Fund. Mol. M. 623 (2007) 53–71.
[14] D. Bandyopadhyay, J.C. Granados, J.D. Short, B.K. Banik, Polycyclic aromatic compounds as anticancer agents: evaluation of synthesis and in vitro cytotoxicity, Oncol. Lett. 3 (2012) 45–49.
[15] R. Martínez, L. Chacón-García, The search of DNA-intercalators as antitumoral drugs: what it worked and what did not work, Curr. Med. Chem. 12 (2005) 127–151.
[16] A.C. Gentry, S. Juul, C. Veigaard, B.R. Knudsen, N. Osheroff, The geometry of DNA supercoils modulates the DNA cleavage activity of human topoisomerase I, Nucl. Acids Res. 39 (2011) 1014–1022.
[17] M.R. Webb, S.E. Ebeler, Comparative analysis of topoisomerase IB inhibition and DNA intercalation by flavonoids and similar compounds: structural determinates of activity, Biochem. J. 384 (2004) 527–541.
[18] H. Torigoe, S. Sato, K. Yamashita, S. Obika, T. Imanishi, S. Takenaka, Binding of threading intercalator to nucleic acids: thermodynamic analyses, Nucl. Acids Res. Suppl. 2 (2002) 55–56.
[19] L. Strekowski, B. Wilson, Noncovalent interactions with DNA: an overview, Mutat. Res. -Fund. Mol. M. 623 (2007) 3–13.
[20] S.F. Yen, E.J. Gabbay, W.D. Wilson, Interaction of aromatic imides with DNA. 1. Spectrophotometric and viscometric studies, Biochemistry 21 (1982) 2070–2076.
[21] F.A. Tanious, S.F. Yen, W.D. Wilson, Kinetic and equilibrium analysis of a threading intercalation mode: DNA sequence and ion effects, Biochemistry 30 (1991) 1813–1819.
[22] H.-K. Liu, P.J. Sadler, Metal complexes as DNA intercalators, Acc. Chem. Res. 44 (2011) 349–359.
[23] W.A. Denny, Acridine derivatives as chemotherapeutic agents, Curr. Med. Chem. 9 (2002) 1655–1665.
[24] W. Henry david, Adriamycin, in: Cancer Chemotherapy, American Chemical Society, 1976, pp. 15–57.
[25] W.J. Pigram, W. Fuller, L.D. Hamilton, Stereochemistry of intercalation: interaction of daunomycin with DNA, Nature 235 (1972) 17–19.
[26] G.J. Quigley, A.H. Wang, G. Ughetto, G. van der Marel, J.H. van Boom, A. Rich, Molecular structure of an anticancer drug–DNA complex: daunomycin plus d(CpGpTpApCpG), Proc. Natl. Acad. Sci. U. S. A. 77 (1980) 7204–7208.
[27] H.M. Sobell, B.S. Reddy, K.K. Bhandary, S.C. Jain, T.D. Sakore, T.P. Seshadri, Conformational flexibility in DNA structure as revealed by structural studies of drug intercalation and its broader implications in understanding the organization of DNA in chromatin, Cold Spring Harb. Symp. Quant. Biol. 42 (Pt 1) (1978) 87–102.
[28] K. Van Dyke, C. Lantz, C. Szustkiewicz, Quinacrine: mechanisms of antimalarial action, Science 169 (1970) 492–493.
[29] W. Müller, D.M. Crothers, Studies of the binding of actinomycin and related compounds to DNA, J. Mol. Biol. 35 (1968) 251–290.
[30] W.D. Wilson, R.L. Jones, Intercalating drugs: DNA binding and molecular pharmacology, in: A.G. Silvio Garattini (Ed.), Advances in Pharmacology, Academic Press, 1981, pp. 177–222.
[31] M.P. Maguire, K.R. Sheets, K. McVety, A.P. Spada, A. Zilberstein, A new series of PDGF receptor tyrosine kinase inhibitors: 3-substituted quinoline derivatives, J. Med. Chem. 37 (1994) 2129–2137.
[32] D. Dubé, M. Blouin, C. Brideau, C.C. Chan, S. Desmarais, D. Ethier, et al., Quinolines as potent 5-lipoxygenase inhibitors: synthesis and biological profile of L-746,530, Bioorg. Med. Chem. Lett. 8 (1998) 1255–1260.
[33] Y.L. Chen, K.C. Fang, J.Y. Sheu, S.L. Hsu, C.C. Tzeng, Synthesis and antibacterial evaluation of certain quinolone derivatives, J. Med. Chem. 44 (2001) 2374–2377.
[34] B. Gatto, G. Capranico, M. Palumbo, Drugs acting on DNA topoisomerases: recent advances and future perspectives, Curr. Pharm. Des. 5 (1999) 195–215.
[35] T. Aravinda, H.S.B. Naik, H.R.P. Naik, 1,2,3-Triazole fused quinoline-peptidomimetics: studies on synthesis, DNA binding and photonuclease activity, Int. J. Pept. Res. Ther. 15 (2009) 273–279.
[36] F. Fazio, M.C. Bryan, O. Blixt, J.C. Paulson, C.-H. Wong, Synthesis of sugar arrays in microtiter plate, J. Am. Chem. Soc. 124 (2002) 14397–14402.
[37] A. Padwa, 1,3-Dipolar Cycloaddition Chemistry, Wiley, New York, 1984.
[38] H.R. Prakash Naik, H.S. Bhojya Naik, T.R. Ravikumar Naik, H.R. Naik, D.S. Lamani, T. Aravinda, Pyrimido[4,5-b]quinoline-2-thiol/ol: microwave-induced one-pot synthesis, DNA binding and cleavage studies, J. Sulfur Chem. 29 (2008) 583–592.
[39] R. Palchaudhuri, P.J. Hergenrother, DNA as a target for anticancer compounds: methods to determine the mode of binding and the mechanism of action, Curr. Opin. Biotechnol. 18 (2007) 497–503.
[40] A. Garofalo, L. Goossens, B. Baldeyrou, A. Lemoine, S. Ravez, P. Six, et al., Design, synthesis, and DNA-binding of *N*-alkyl(anilino)quinazoline derivatives, J. Med. Chem. 53 (2010) 8089–8103.
[41] B. Nordén, F. Tjerneld, Structure of methylene blue–DNA complexes studied by linear and circular dichroism spectroscopy, Biopolymers 21 (1982) 1713–1734.
[42] S. Sharma, K. Panjamurthy, B. Choudhary, M. Srivastava, M. Shahabuddin, R. Giri, et al., A novel DNA intercalator, 8-methoxy pyrimido[4′,5′:4,5]thieno(2,3-b)quinoline-4(3*H*)-one induces apoptosis in cancer cells, inhibits the tumor progression and enhances lifespan in mice with tumor, Mol. Carcinog. 52 (2013) 413–425.
[43] M.S. Shahabuddin, M. Nambiar, G.M. Advirao, S.C. Raghavan, Intercalative pyrimido[4′,5′:4,5]thieno(2,3-b)quinolines induce apoptosis in leukemic cells: a comparative study of methoxy and morpholino substitution, Invest. New Drugs 29 (2011) 873–882.
[44] M.S. Shahabuddin, M. Nambiar, B. Choudhary, G.M. Advirao, S.C. Raghavan, A novel DNA intercalator, butylamino-pyrimido[4′,5′:4,5]selenolo(2,3-b) quinoline, induces cell cycle arrest and apoptosis in leukemic cells, Invest. New Drugs 28 (2010) 35–48.
[45] K. El-Bayoumy, R. Sinha, Mechanisms of mammary cancer chemoprevention by organoselenium compounds, Mutat. Res. -Fund. Mol. M. 551 (2004) 181–197.
[46] C.-H. Tseng, C.-C. Tzeng, K.-Y. Chung, C.-L. Kao, C.-Y. Hsu, C.-M. Cheng, et al., Synthesis and antiproliferative evaluation of 6-aryl-11-iminoindeno[1,2-*c*] quinoline derivatives, Bioorg. Med. Chem. 19 (2011) 7653–7663.
[47] C.-H. Tseng, Y.-L. Chen, C.-L. Yang, C.-M. Cheng, C.-H. Han, C.-C. Tzeng, Synthesis of 6-substituted 9-methoxy-11*H*-indeno[1,2-*c*]quinoline-11-one derivatives as potential anticancer agents, Bioorg. Med. Chem. 20 (2012) 4397–4404.
[48] E. Kuruvilla, J. Joseph, D. Ramaiah, Novel bifunctional acridine–acridinium conjugates: synthesis and study of their chromophore-selective electron-transfer and DNA-binding properties, J. Phys. Chem. B 109 (2005) 21997–22002.
[49] W. Li, Z.-W. Zhang, S.-X. Wang, S.-M. Ren, T. Jiang, Synthesis and analysis of potential DNA intercalators containing quinoline–glucose hybrids, Chem. Biol. Drug Des. 74 (2009) 80–86.
[50] T. Wunberg, C. Kallus, T. Opatz, S. Henke, W. Schmidt, H. Kunz, Carbohydrates as multifunctional chiral scaffolds in combinatorial synthesis, Angew. Chem. Int. Ed. 37 (1998) 2503–2505.
[51] Y.-F. Song, P. Yang, Mononuclear tetrapyrido[3,2-a:2′,3′-c:3″,2″-h:2‴,3‴-j] phenazine (tpphz) cobalt complex, Polyhedron 20 (2001) 501–506.
[52] Q. Zhang, F. Zhang, W. Wang, X. Wang, Synthesis, crystal structure and DNA binding studies of a binuclear copper(II) complex with phenanthroline, J. Inorg. Biochem. 100 (2006) 1344–1352.
[53] N.S. Hari Narayana Moorthy, C. Karthikeyan, P. Trivedi, Synthesis, cytotoxic evaluation and in silico pharmacokinetic prediction of some benzo[a]phenazine-5-sulfonic acid derivatives, Med. Chem. 5 (2009) 549–557.
[54] C.A. Lipinski, Lead- and drug-like compounds: the rule-of-five revolution, Drug Discovery Today Technol. 1 (2004) 337–341.
[55] X. Li, Q. Wang, Y. Qing, Y. Lin, Y. Zhang, X. Qian, et al., Novel DNA intercalators without basic side chains as efficient antitumor agents: design, synthesis and evaluation of benzo-[c,d]-indol-malononitrile derivatives, Bioorg. Med. Chem. 18 (2010) 3279–3284.
[56] P.T. Selvi, M. Palaniandavar, Spectral, viscometric and electrochemical studies on mixed ligand cobalt(III) complexes of certain diimine ligands bound to calf thymus DNA, Inorg. Chim. Acta 337 (2002) 420–428.
[57] H. Ihmels, D. Otto, Intercalation of organic dye molecules into double-stranded DNA – general principles and recent developments, in: F. Würthner (Ed.), Supermolecular Dye Chemistry, Springer, Berlin Heidelberg, 2005, pp. 161–204.
[58] K. Nakatani, C. Dohno, T. Nakamura, I. Saito, *p*-Cyano substituted benzophenone as an excellent photophore for one-electron oxidation of DNA, Tetrahedron Lett. 39 (1998) 2779–2782.
[59] R. Dallocchio, A. Dessi, V. Sanna, N. Pala, I. Campesi, G. Paglietti, et al., DNA binders: 2. Molecular recognition of DNA by 2,3,6,7-tetrahydro-1*H*pyrrolo [1,2-*a*]indole-1,8(5*H*)-dione bis(4,5-dihydro-1*H*-imidazol-2-ylhydrazone) as a prototype of two-armed intercalating agents, Lett. Drug. Des. Discovery 6 (2009) 246–251.
[60] J.-H. Lin, A.L. Perryman, J.R. Schames, J.A. McCammon, Computational drug design accommodating receptor flexibility: the relaxed complex scheme, J. Am. Chem. Soc. 124 (2002) 5632–5633.
[61] J.-H. Lin, A.L. Perryman, J.R. Schames, J.A. McCammon, The relaxed complex method: accommodating receptor flexibility for drug design with an improved scoring scheme, Biopolymers 68 (2003) 47–62.
[62] J.A. McCammon, Target flexibility in molecular recognition, Biochim. Biophys. Acta 1754 (2005) 221–224.
[63] R.B. Macgregor, R.M. Clegg, T.M. Jovin, Viscosity dependence of ethidium-DNA intercalation kinetics, Biochemistry 26 (1987) 4008–4016.
[64] M. Zhao, L. Bi, W. Wang, C. Wang, M. Baudy-Floc'h, J. Ju, et al., Synthesis and cytotoxic activities of beta-carboline amino acid ester conjugates, Bioorg. Med. Chem. 14 (2006) 6998–7010.
[65] J. Wu, M. Zhao, K. Qian, K.-H. Lee, S. Morris-Natschke, S. Peng, Novel *N*-(3-carboxyl-9-benzyl-beta-carboline-1-yl)ethylamino acids: synthesis, antitumor evaluation, intercalating determination, 3D QSAR analysis and docking investigation, Eur. J. Med. Chem. 44 (2009) 4153–4161.

[66] C.A. Hastings, J.K. Barton, Perturbing the DNA sequence selectivity of metallointercalator–peptide conjugates by single amino acid modification, Biochemistry 38 (1999) 10042–10051.
[67] H. Han, R.L. de Vrueh, J.K. Rhie, K.M. Covitz, P.L. Smith, C.P. Lee, et al., 5′-Amino acid esters of antiviral nucleosides, acyclovir, and AZT are absorbed by the intestinal PEPT1 peptide transporter, Pharm. Res. 15 (1998) 1154–1159.
[68] M.E. Ganapathy, W. Huang, H. Wang, V. Ganapathy, F.H. Leibach, Valacyclovir: a substrate for the intestinal and renal peptide transporters PEPT1 and PEPT2, Biochem. Biophys. Res. Commun. 246 (1998) 470–475.
[69] X. Zhang, Y. Yang, M. Zhao, L. Liu, M. Zheng, Y. Wang, et al., A class of Trp-Trp-AA-OBzl: synthesis, in vitro anti-proliferation/in vivo anti-tumor evaluation, intercalation-mechanism investigation and 3D QSAR analysis, Eur. J. Med. Chem. 46 (2011) 3410–3419.
[70] A.M. Sobhani, S.R. Amini, J.D.A. Tyndall, E. Azizi, M. Daneshtalab, A. Khalaj, A theory of mode of action of azolylalkylquinolines as DNA binding agents using automated flexible ligand docking, J. Mol. Graph. Modell. 25 (2006) 459–469.
[71] C.M. Venkatachalam, X. Jiang, T. Oldfield, M. Waldman, LigandFit: a novel method for the shape-directed rapid docking of ligands to protein active sites, J. Mol. Graph. Modell. 21 (2003) 289–307.
[72] J. Wu, C. Li, M. Zhao, W. Wang, Y. Wang, S. Peng, A class of novel carboline intercalators: their synthesis, in vitro anti-proliferation, in vivo anti-tumor action, and 3D QSAR analysis, Bioorg. Med. Chem. 18 (2010) 6220–6229.
[73] L. Tan, J. Shen, J. Liu, L. Zeng, L. Jin, C. Weng, Spectral characteristics, DNA-binding and cytotoxicity of two functional Ru(II) mixed-ligand complexes, Dalton Trans. 41 (2012) 4575–4587.
[74] J.-L. Mergny, L. Lacroix, Analysis of thermal melting curves, Oligonucleotides 13 (2003) 515–537.
[75] S.A. Gamage, N. Tepsiri, P. Wilairat, S.J. Wojcik, D.P. Figgitt, R.K. Ralph, et al., Synthesis and in vitro evaluation of 9-anilino-3,6-diaminoacridines active against a multidrug-resistant strain of the malaria parasite *Plasmodium falciparum*, J. Med. Chem. 37 (1994) 1486–1494.
[76] R. Guddneppanavar, G. Saluta, G.L. Kucera, U. Bierbach, Synthesis, biological activity, and DNA-damage profile of platinum-threading intercalator conjugates designed to target adenine, J. Med. Chem. 49 (2006) 3204–3214.
[77] M. Wainwright, Acridine – a neglected antibacterial chromophore, J. Antimicrob. Chemother. 47 (2001) 1–13.
[78] L.R. Ferguson, W.A. Denny, Genotoxicity of non-covalent interactions: DNA intercalators, Mutat. Res. 623 (2007) 14–23.
[79] P. Belmont, I. Dorange, Acridine/acridone: a simple scaffold with a wide range of application in oncology, Expert Opin. Ther. Pat. 18 (2008) 1211–1224.
[80] W.R. Wilson, W.A. Denny, S.J. Twigden, B.C. Baguley, J.C. Probert, Selective toxicity of nitracrine to hypoxic mammalian cells, Br. J. Cancer 49 (1984) 215–223.
[81] J.W. Paxton, J.L. Jurlina, S.E. Foote, The binding of amsacrine to human plasma proteins, J. Pharm. Pharmacol. 38 (1986) 432–438.
[82] W.R. Grove, C.L. Fortner, P.H. Wiernik, Review of amsacrine, an investigational antineoplastic agent, Clin. Pharm. 1 (1982) 320–326.
[83] A.C. Ketron, W.A. Denny, D.E. Graves, N. Osheroff, Amsacrine as a topoisomerase II poison: importance of drug–DNA interactions, Biochemistry 51 (2012) 1730–1739.
[84] S. Vispé, I. Vandenberghe, M. Robin, J.P. Annereau, L. Créancier, V. Pique, et al., Novel tetra-acridine derivatives as dual inhibitors of topoisomerase II and the human proteasome, Biochem. Pharmacol. 73 (2007) 1863–1872.
[85] B.H. Nicholson, A.R. Peacocke, The inhibition of ribonucleic acid polymerase by acridines, Biochem. J. 100 (1966) 50–58.
[86] C.-W. Shiau, C.-C. Yang, S.K. Kulp, K.-F. Chen, C.-S. Chen, J.-W. Huang, et al., Thiazolidenediones mediate apoptosis in prostate cancer cells in part through inhibition of Bcl-xL/Bcl-2 functions independently of PPARgamma, Cancer Res. 65 (2005) 1561–1569.
[87] W. Li, Y. Lu, Z. Wang, J.T. Dalton, D.D. Miller, Synthesis and antiproliferative activity of thiazolidine analogs for melanoma, Bioorg. Med. Chem. Lett. 17 (2007) 4113–4117.
[88] L. Janovec, M. Kožurková, D. Sabolová, J. Ungvarský, H. Paulíková, J. Plšíková, et al., Cytotoxic 3,6-bis((imidazolidinone)imino)acridines: synthesis, DNA binding and molecular modeling, Bioorg. Med. Chem. 19 (2011) 1790–1801.
[89] F.W.A. Barros, T.G. Silva, M.G. da Rocha Pitta, D.P. Bezerra, L.V. Costa-Lotufo, M.O. de Moraes, et al., Synthesis and cytotoxic activity of new acridine-thiazolidine derivatives, Bioorg. Med. Chem. 20 (2012) 3533–3539.
[90] F.Q. Schafer, G.R. Buettner, Redox environment of the cell as viewed through the redox state of the glutathione disulfide/glutathione couple, Free Radical Biol. Med. 30 (2001) 1191–1212.
[91] F.V. Pallardó, J. Markovic, J.L. García, J. Viña, Role of nuclear glutathione as a key regulator of cell proliferation, Mol. Asp. Med. 30 (2009) 77–85.
[92] H. Paulíková, Z. Vantová, L. Hunáková, L. Čižeková, M. Čarná, M. Kožurková, et al., DNA binding acridine-thiazolidinone agents affecting intracellular glutathione, Bioorg. Med. Chem. 20 (2012) 7139–7148.
[93] S. Cicchi, A. Goti, A. Brandi, A. Guarna, F. De Sarlo, 1,3-Aminoalcohols by reductive cleavage of isoxazolidines with molybdenum hexacarbonyl, Tetrahedron Lett. 31 (1990) 3351–3354.
[94] S. Usha, I.M. Johnson, R. Malathi, Interaction of resveratrol and genistein with nucleic acids, J. Biochem. Mol. Biol. 38 (2005) 198–205.
[95] A. Favier, M. Blackledge, J.P. Simorre, S. Crouzy, V. Dabouis, A. Gueiffier, et al., Solution structure of 2-(pyrido[1,2-*e*]purin-4-yl)amino-ethanol intercalated in the DNA duplex d(CGATCG)2, Biochemistry 40 (2001) 8717–8726.
[96] L. Von Szentpaly, I.L. Shamovsky, Molecular mechanics explanation for the stereochemical and shape selectivity of B-DNA for "bay-region" carcinogens, Mol. Pharmacol. 47 (1995) 624–629.
[97] B.K. Vishu Kumar, K. Dhananjaya, K.S. Rangappa, Synthesis, characterization, and biological studies of novel isoxazolidines: 1,3-dipolar cycloaddition reactions, Synth. Commun. 32 (2002) 1887–1890.
[98] F. Pasternack Robert, J. Gibbs Esther, Interaction of porphyrins and Metalloporphyrins with nucleic acids, in: Metal-DNA Chemistry, American Chemical Society, 1989, pp. 59–73.
[99] A. Rescifina, M.A. Chiacchio, A. Corsaro, E. De Clercq, D. Iannazzo, A. Mastino, et al., Synthesis and biological activity of isoxazolidinyl polycyclic aromatic hydrocarbons: potential DNA intercalators, J. Med. Chem. 49 (2006) 709–715.
[100] A. Rescifina, U. Chiacchio, A. Piperno, S. Sortino, Binding of a non-ionic pyrenylisoxazolidine derivative to double-stranded polynucleotides: spectroscopic and molecular modelling studies, New J. Chem. 30 (2006) 554.
[101] A. Rescifina, U. Chiacchio, A. Corsaro, A. Piperno, R. Romeo, Isoxazolidinyl polycyclic aromatic hydrocarbons as DNA-intercalating antitumor agents, Eur. J. Med. Chem. 46 (2011) 129–136.
[102] A. Rescifina, M.G. Varrica, C. Carnovale, G. Romeo, U. Chiacchio, Novel isoxazole polycyclic aromatic hydrocarbons as DNA-intercalating agents, Eur. J. Med. Chem. 51 (2012) 163–173.
[103] A. Ono, S. Cao, H. Togashi, M. Tashiro, T. Fujimoto, T. Machinami, et al., Specific interactions between silver(I) ions and cytosine-cytosine pairs in DNA duplexes, Chem. Commun. (Camb.) (2008) 4825–4827.
[104] A. Rescifina, C. Zagni, G. Romeo, S. Sortino, Synthesis and biological activity of novel bifunctional isoxazolidinyl polycyclic aromatic hydrocarbons, Bioorg. Med. Chem. 20 (2012) 4978–4984.
[105] M. Egli, L.D. Williams, C.A. Frederick, A. Rich, DNA-nogalamycin interactions, Biochemistry 30 (1991) 1364–1372.
[106] L.D. Williams, M. Egli, G. Qi, P. Bash, G.A. van der Marel, J.H. van Boom, et al., Structure of nogalamycin bound to a DNA hexamer, Proc. Natl. Acad. Sci. U. S. A. 87 (1990) 2225–2229.
[107] L.A. Howell, R. Gulam, A. Mueller, M.A. O'Connell, M. Searcey, Design and synthesis of threading intercalators to target DNA, Bioorg. Med. Chem. Lett. 20 (2010) 6956–6959.
[108] Y. Sun, K. Xun, Y. Wang, X. Chen, A systematic review of the anticancer properties of berberine, a natural product from Chinese herbs, Anticancer Drugs 20 (2009) 757–769.
[109] D.S. Pilch, C. Yu, D. Makhey, E.J. LaVoie, A.R. Srinivasan, W.K. Olson, et al., Minor groove-directed and intercalative ligand–DNA interactions in the poisoning of human DNA topoisomerase I by protoberberine analogs, Biochemistry 36 (1997) 12542–12553.
[110] P. Krishnan, K.F. Bastow, The 9-position in berberine analogs is an important determinant of DNA topoisomerase II inhibition, Anticancer Drugs Des. 15 (2000) 255–264.
[111] A. Basu, P. Jaisankar, G. Suresh Kumar, Synthesis of novel 9-*O*-*N*-aryl/arylalkyl amino carbonyl methyl substituted berberine analogs and evaluation of DNA binding aspects, Bioorg. Med. Chem. 20 (2012) 2498–2505.
[112] J.B. Hansen, P. Bjerring, O. Buchardt, P. Ebbesen, A. Kanstrup, G. Karup, et al., Psoralenamines. 3. Synthesis, pharmacological behavior, and DNA binding of 5-(aminomethyl)-8-methoxy-, 5-[[(3-aminopropyl)oxy]methyl]-, and 8-[(3-aminopropyl)oxy]psoralen derivatives, J. Med. Chem. 28 (1985) 1001–1010.
[113] M. Yamada, M. Inoue, T. Yamada, Synthesis of DNA intercalator–immobilized cyclodextrin and interaction with double-stranded DNA: utilization of DNA–cyclodextrin conjugated material as an environmental remediation material, Polym. Chem. 3 (2012) 1291–1299.
[114] S. Kawanishi, Y. Hiraku, Amplification of anticancer drug-induced DNA damage and apoptosis by DNA-binding compounds, Curr. Med. Chem. Anticancer Agents 4 (2004) 415–419.
[115] B. Gyurcsik, A. Czene, Towards artificial metallonucleases for gene therapy: recent advances and new perspectives, Future Med. Chem. 3 (2011) 1935–1966.
[116] X. Sheng, X.-M. Lu, Y.-T. Chen, G.-Y. Lu, J.-J. Zhang, Y. Shao, et al., Synthesis, DNA-binding, cleavage, and cytotoxic activity of new 1,7-dioxa-4,10-diazacyclododecane artificial receptors containing bisguanidinoethyl or diaminoethyl double side arms, Chemistry 13 (2007) 9703–9712.
[117] Y. Shao, X. Sheng, Y. Li, Z.-L. Jia, J.-J. Zhang, F. Liu, et al., DNA binding and cleaving activity of the new cleft molecule N,N′-bis(guanidinoethyl)-2,6-pyridinedicarboxamide in the absence or in the presence of copper(II), Bioconjugate Chem. 19 (2008) 1840–1848.
[118] B. Gruber, E. Kataev, J. Aschenbrenner, S. Stadlbauer, B. König, Vesicles and micelles from amphiphilic zinc(II)-cyclen complexes as highly potent promoters of hydrolytic DNA cleavage, J. Am. Chem. Soc. 133 (2011) 20704–20707.
[119] L. Wei, Y. Shao, M. Zhou, H.-W. Hu, G.-Y. Lu, Synthesis and enhanced DNA cleavage activities of bis-tacnorthoamide derivatives, Org. Biomol. Chem. 10 (2012) 8484–8492.
[120] J. Portugal, Chartreusin, elsamicin A and related anti-cancer antibiotics, Curr. Med. Chem. Anticancer Agents 3 (2003) 411–420.
[121] A. Lorico, B.H. Long, Biochemical characterisation of elsamicin and other coumarin-related antitumour agents as potent inhibitors of human topoisomerase II, Eur. J. Cancer 29A (1993) 1985–1991.

[122] N. Ueberschaar, H.-M. Dahse, T. Bretschneider, C. Hertweck, Rational design of an apoptosis-inducing photoreactive DNA intercalator, Angew. Chem. Int. Ed. Engl. 52 (2013) 6185–6189.
[123] G. Wang, H. Wu, D. Wang, C. Yan, Y. Lu, Exploring the binding mechanism of phosphoramidate derivative with DNA: spectroscopy, calorimetry and modeling, Spectrochim. Acta A Mol. Biomol. Spectrosc. 104 (2013) 492–496.
[124] P. Paul, M. Hossain, R.C. Yadav, G.S. Kumar, Biophysical studies on the base specificity and energetics of the DNA interaction of photoactive dye thionine: spectroscopic and calorimetric approach, Biophys. Chem. 148 (2010) 93–103.
[125] J. Andersson, S. Li, P. Lincoln, J. Andréasson, Photoswitched DNA-binding of a photochromic spiropyran, J. Am. Chem. Soc. 130 (2008) 11836–11837.
[126] A. Mammana, G.T. Carroll, J. Areephong, B.L. Feringa, A chiroptical photoswitchable DNA complex, J. Phys. Chem. B 115 (2011) 11581–11587.
[127] C. Dohno, T. Yamamoto, K. Nakatani, Photoswitchable unsymmetrical ligand for DNA hetero-mismatches, Eur. J. Org. Chem. 2009 (2009) 4051–4058.
[128] S.V. Paramonov, V. Lokshin, H. Ihmels, O.A. Fedorova, Influence of DNA-binding on the photochromic equilibrium of a chromene derivative, Photochem. Photobiol. Sci. 10 (2011) 1279–1282.
[129] M. Hranjec, B. Lučić, I. Ratkaj, S.K. Pavelić, I. Piantanida, K. Pavelić, et al., Novel imidazo[4,5-b]pyridine and triaza-benzo[c]fluorene derivatives: synthesis, antiproliferative activity and DNA binding studies, Eur. J. Med. Chem. 46 (2011) 2748–2758.
[130] H. Ihmels, J. Mattay, F. May, L. Thomas, Photoswitchable DNA-binding properties of a photochromic spirooxazine derivative, Org. Biomol. Chem. 11 (2013) 5184–5188.
[131] D. Berdnikova, O. Fedorova, E. Gulakova, H. Ihmels, Photoinduced in situ generation of a DNA-binding benzothiazoloquinolinium derivative, Chem. Commun. 48 (2012) 4603–4605.
[132] W.A. Denny, Acridine-4-carboxamides and the concept of minimal DNA intercalators, in: Martine Demeunynck, C. Bailly, W.D. Wilson (Eds.), Small Molecule DNA and RNA Binders, Wiley-VCH Verlag GmbH & Co. KGaA, 2004, pp. 482–502.
[133] G.E.P. Box, N.R. Draper, Empirical Model-building and Response Surfaces, Wiley, 1987.
[134] M. Orozco, A. Noy, A. Pérez, Recent advances in the study of nucleic acid flexibility by molecular dynamics, Curr. Opin. Struct. Biol. 18 (2008) 185–193.
[135] N. Moitessier, P. Englebienne, D. Lee, J. Lawandi, C.R. Corbeil, Towards the development of universal, fast and highly accurate docking/scoring methods: a long way to go, Br. J. Pharmacol. 153 (Suppl. 1) (2008) S7–S26.
[136] P.A. Holt, J.B. Chaires, J.O. Trent, Molecular docking of intercalators and groove-binders to nucleic acids using Autodock and Surflex, J. Chem. Inf. Modell. 48 (2008) 1602–1615.
[137] C.G. Ricci, P.A. Netz, Docking studies on DNA–ligand interactions: building and application of a protocol to identify the binding mode, J. Chem. Inf. Modell. 49 (2009) 1925–1935.
[138] X.-J. Lu, W.K. Olson, 3DNA: a software package for the analysis, rebuilding and visualization of three-dimensional nucleic acid structures, Nucl. Acids Res. 31 (2003) 5108–5121.
[139] A. Pérez, I. Marchán, D. Svozil, J. Sponer, T.E. Cheatham 3rd, C.A. Laughton, et al., Refinement of the AMBER force field for nucleic acids: improving the description of alpha/gamma conformers, Biophys. J. 92 (2007) 3817–3829.
[140] P. Várnai, K. Zakrzewska, DNA and its counterions: a molecular dynamics study, Nucl. Acids Res. 32 (2004) 4269–4280.
[141] H. Wang, C. Laughton, Molecular modelling methods for prediction of sequence-selectivity in DNA recognition, Methods 42 (2007) 196–203.
[142] D.L. Beveridge, T.E. Cheatham 3rd, M. Mezei, The ABCs of molecular dynamics simulations on B-DNA, circa 2012, J. Biosci. 37 (2012) 379–397.
[143] A. Pérez, F.J. Luque, M. Orozco, Frontiers in molecular dynamics simulations of DNA, Acc. Chem. Res. 45 (2012) 196–205.
[144] R.B. Macgregor Jr., R.M. Clegg, T.M. Jovin, Pressure-jump study of the kinetics of ethidium bromide binding to DNA, Biochemistry 24 (1985) 5503–5510.
[145] L.P. Wakelin, M.J. Waring, Kinetics of drug–DNA interaction. Dependence of the binding mechanism on structure of the ligand, J. Mol. Biol. 144 (1980) 183–214.
[146] F.J. Meyer-Almes, D. Porschke, Mechanism of intercalation into the DNA double helix by ethidium, Biochemistry 32 (1993) 4246–4253.
[147] F. Leng, J.B. Chaires, M.J. Waring, Energetics of echinomycin binding to DNA, Nucl. Acids Res. 31 (2003) 6191–6197.
[148] D.P. Ryan, D.M. Crothers, Relaxation kinetics of DNA–ligand binding including direct transfer, Biopolymers 23 (1984) 537–562.
[149] J.L. Bresloff, D.M. Crothers, DNA–ethidium reaction kinetics: demonstration of direct ligand transfer between DNA binding sites, J. Mol. Biol. 95 (1975) 103–123.
[150] J.B. Chaires, N. Dattagupta, D.M. Crothers, Kinetics of the daunomycin–DNA interaction, Biochemistry 24 (1985) 260–267.
[151] V. Rizzo, N. Sacchi, M. Menozzi, Kinetic studies of anthracycline–DNA interaction by fluorescence stopped flow confirm a complex association mechanism, Biochemistry 28 (1989) 274–282.
[152] J. Luo, T.C. Bruice, Ten-nanosecond molecular dynamics simulation of the motions of the horse liver alcohol dehydrogenase.PhCH$_2$O– complex, Proc. Natl. Acad. Sci. U. S. A. 99 (2002) 16597–16600.
[153] F. Rao, A. Caflisch, Replica exchange molecular dynamics simulations of reversible folding, J. Chem. Phys. 119 (2003) 4035–4042.
[154] R.A. Böckmann, H. Grubmüller, Nanoseconds molecular dynamics simulation of primary mechanical energy transfer steps in F1-ATP synthase, Nat. Struct. Biol. 9 (2002) 198–202.
[155] A. Laio, M. Parrinello, Escaping free-energy minima, Proc. Natl. Acad. Sci. USA 99 (2002) 12562–12566.
[156] J. Kästner, Umbrella Sampling, in: Wiley Interdisciplinary Reviews: Computational Molecular Science, vol. 1, 2011, pp. 932–942.
[157] R.R. Monaco, Capture of a transition state using molecular dynamics: creation of an intercalation site in dsDNA with ethidium cation, J. Nucl. Acids 2010 (2010).
[158] The movie of MD simulation was posted in this link: http://www.youtube.com/watch?v=ltSyPPH4T8g.
[159] A. Mukherjee, R. Lavery, B. Bagchi, J.T. Hynes, On the molecular mechanism of drug intercalation into DNA: a simulation study of the intercalation pathway, free Energy, and DNA structural changes, J. Am. Chem. Soc. 130 (2008) 9747–9755.
[160] M. Wilhelm, A. Mukherjee, B. Bouvier, K. Zakrzewska, J.T. Hynes, R. Lavery, Multistep drug intercalation: molecular dynamics and free energy studies of the binding of daunomycin to DNA, J. Am. Chem. Soc. 134 (2012) 8588–8596.
[161] H. Lei, X. Wang, C. Wu, Early stage intercalation of doxorubicin to DNA fragments observed in molecular dynamics binding simulations, J. Mol. Graph. Modell. 38 (2012) 279–289.
[162] W.D. Sasikala, A. Mukherjee, Molecular mechanism of direct proflavine–DNA intercalation: evidence for drug-induced minimum base-stacking penalty pathway, J. Phys. Chem. B 116 (2012) 12208–12212.
[163] W.D. Sasikala, A. Mukherjee, Intercalation and de-intercalation pathway of proflavine through the minor and major grooves of DNA: roles of water and entropy, Phys. Chem. Chem. Phys. 15 (2013) 6446–6455.
[164] H.J. Li, D.M. Crothers, Relaxation studies of the proflavine–DNA complex: the kinetics of an intercalation reaction, J. Mol. Biol. 39 (1969) 461–477.
[165] J. Ramstein, M. Leng, Effect of DNA base composition on the intercalation of proflavine: a kinetic study, Biophys. Chem. 3 (1975) 234–240.